



Self-organized criticality with application to solar flares

Hans Herrmann

Departamento de Física, UFC, Fortaleza, Brazil

and

PMMH, ESPCI Paris

Workshop on Complex Dynamical Systems in Astrophysics
Institute of Fundamental Physics of the Universe
Trieste, February 6-10, 2023



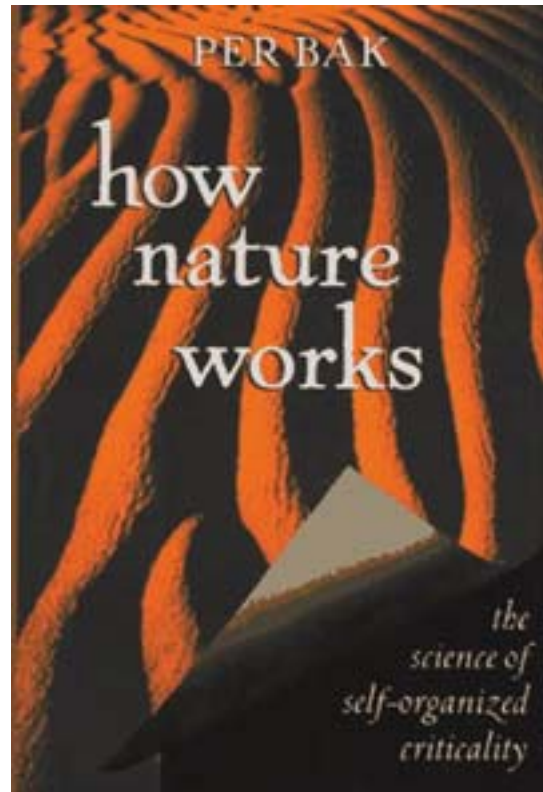
Critical behavior

- Scale-invariance = dilatation symmetry → finite size scaling
- Universality = power-law dependence with exponents that are independent on details
- Asymptotically exact = no deviations in the thermodynamic limit
- No characteristic length scale = correlation length diverges
- Unstable fixed point = small changes in temperature or density will destroy criticality

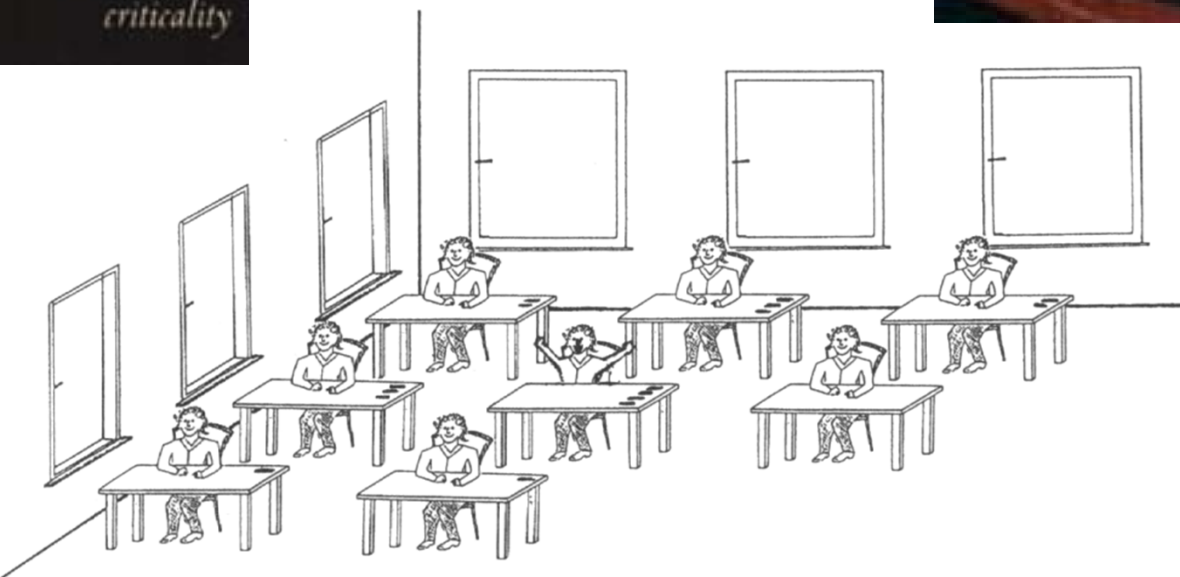


Self-organized criticality

Physique et Mécanique
des Milieux Hétérogènes
UMR 7636



Per Bak
(1948 – 2002)





Self-organized criticality

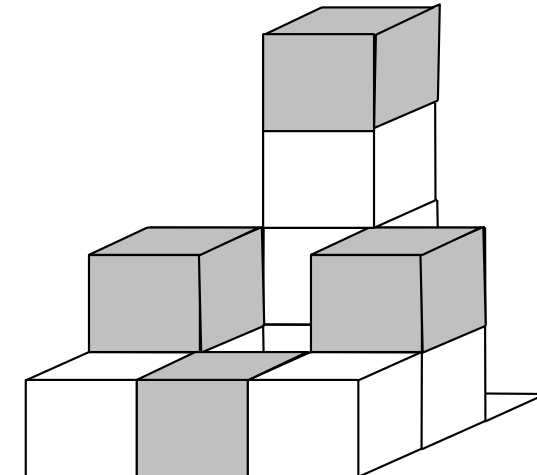
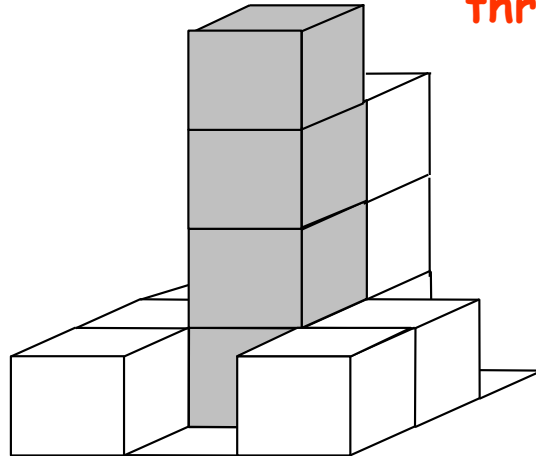
Bak, Tang, Wiesenfeld, PRL 1987

Dynamical systems that evolve spontaneously toward a critical state without parameter tuning → no characteristic event size

Sand pile

by adding at random one grain after another

threshold=4



Fundamental ingredient: separation of time scales

- Slow scale: adding a grain
- Fast scale: propagation of an avalanche

Size and duration
distribution

$$P(s) \sim s^{-1}$$

$$P(T) \sim T^{-0.5}$$

Physique et Mécanique
des Milieux Hétérogènes
UMR 7636

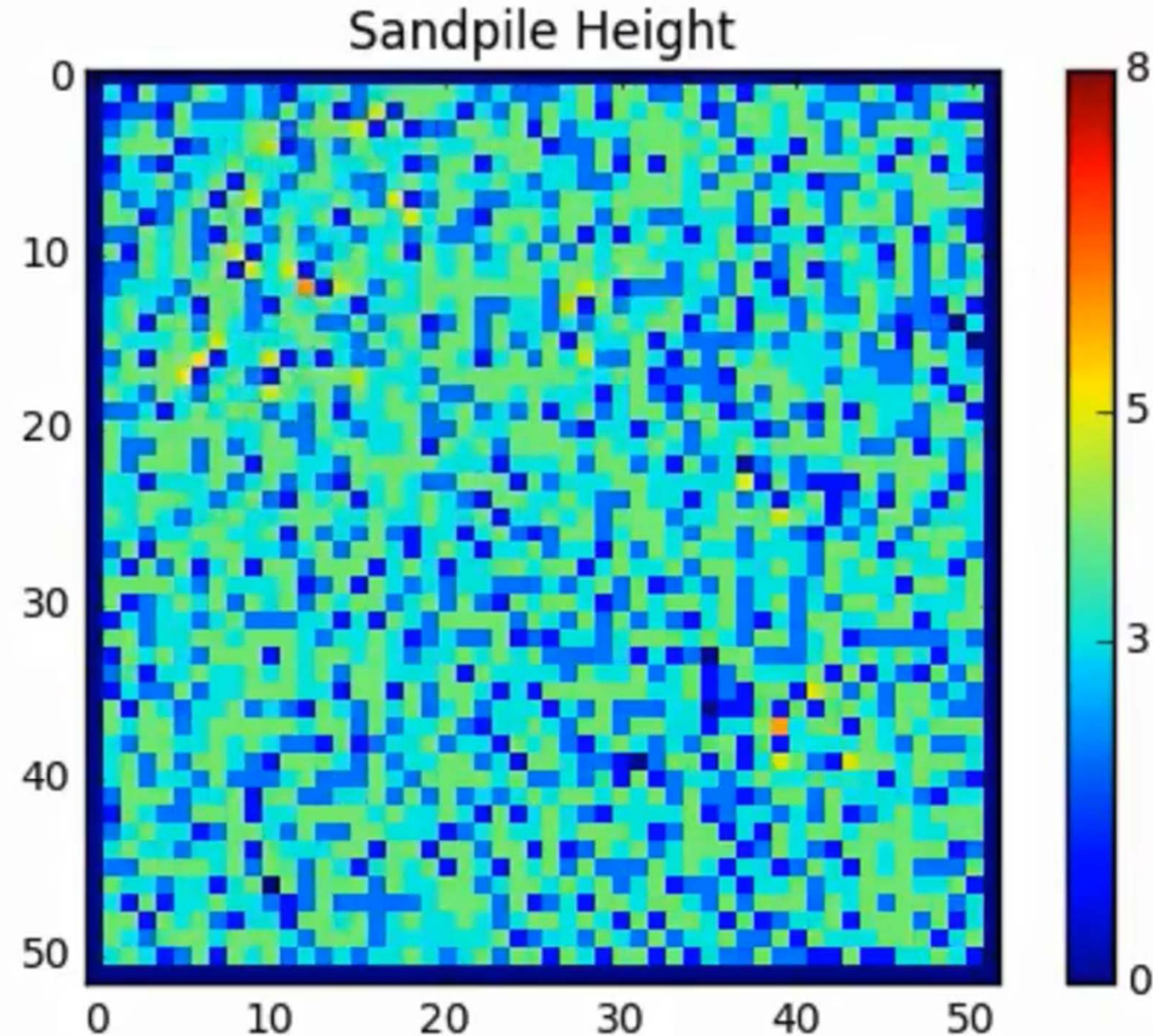




Sand pile model

(Bak, Tang, Wiesenfeld)

Physique et Mécanique
des Milieux Hétérogènes
UMR 7636





SOC variants

Zhang Model (1989)

- Introduces a continuous analog to the BTW sandpile model.
- The sites have continuous energy values between 0 and E_c .

Manna Model (1991)

- Introduces a binary version of the BTW sandpile model.
- The avalanche size and duration exponents are 1.28 and 1.47

Olami-Feder-Christensen (OFC) Model (1992)

Introduces dissipation and was used for solar flares (Hamon et al, 2002)

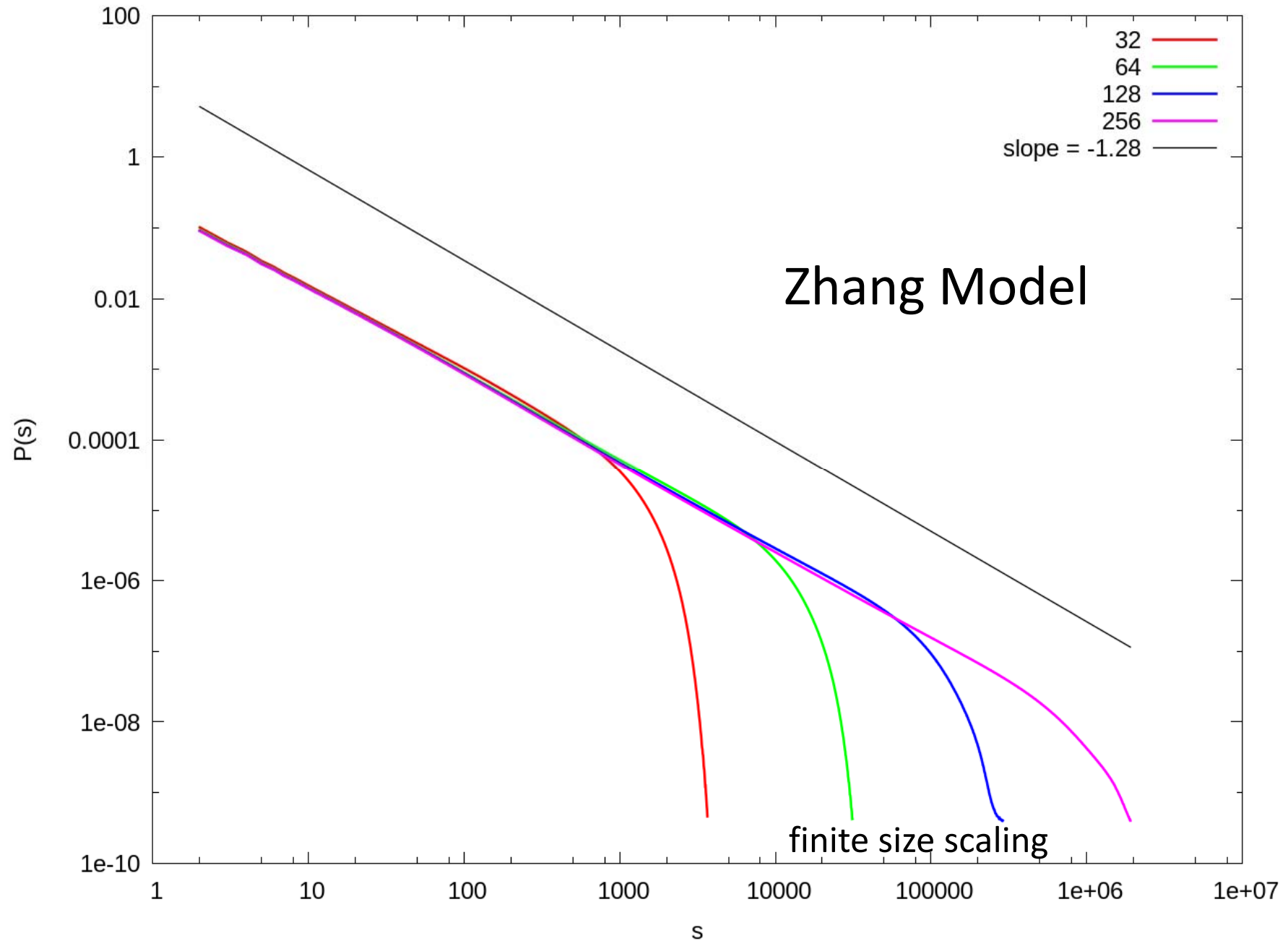
Forest Fire Model (1992)

Bak-Sneppen Model (1993)

threshold dynamics

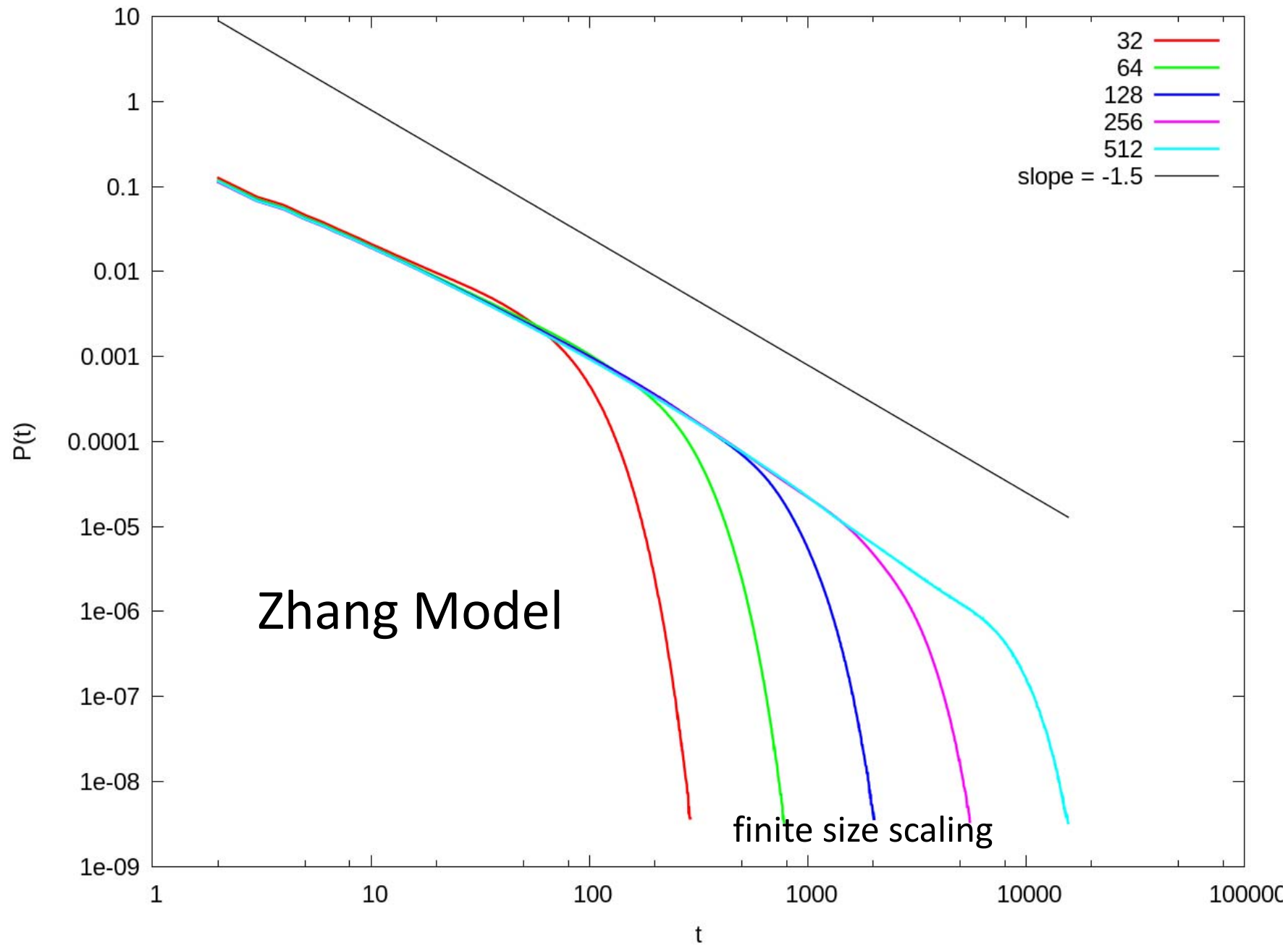


Avalanche Size Distribution





Avalanche Duration Distribution





Possible applications of SOC

Neural avalanches

Invasion percolation

Earthquakes & Shear bands

Solar flares

Reservoir networks

Stock markets

Floods



Turbulence

fully developed and homogeneous turbulence ($\text{Re} \gg 1$)

- Kolmogoroff scaling laws
- Power-law distributions with universal exponents
- No characteristic length scale in the inertial regime
- Self-organized spatio-temporal structure
- Multifractal distribution of vorticity
- Physical length and time scales (dissipation length and inverse Lyapunov exponent)
- Temporal correlations



Scale-free networks

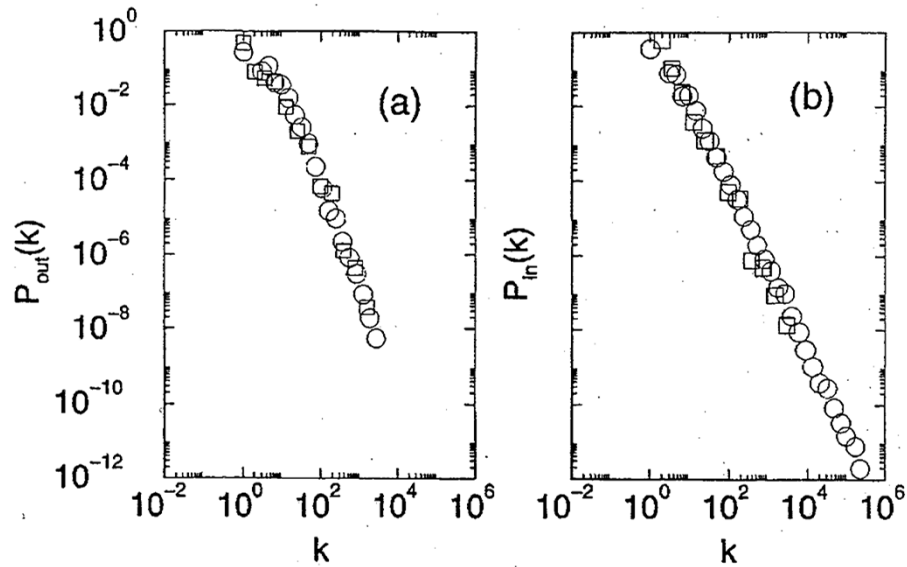
degree-distribution

$$P(k) \propto k^{-\gamma}$$

WWW:

$$\gamma_{out} = 2.4$$

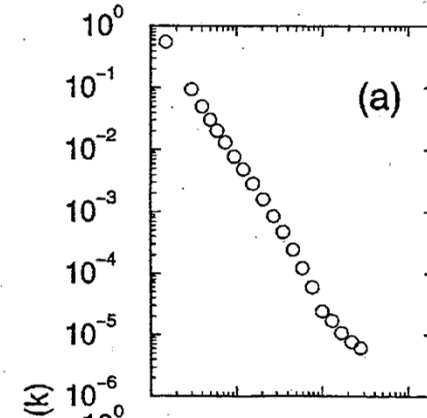
$$\gamma_{in} = 2.1$$



Model: Barabasi-Albert $\gamma = 3$

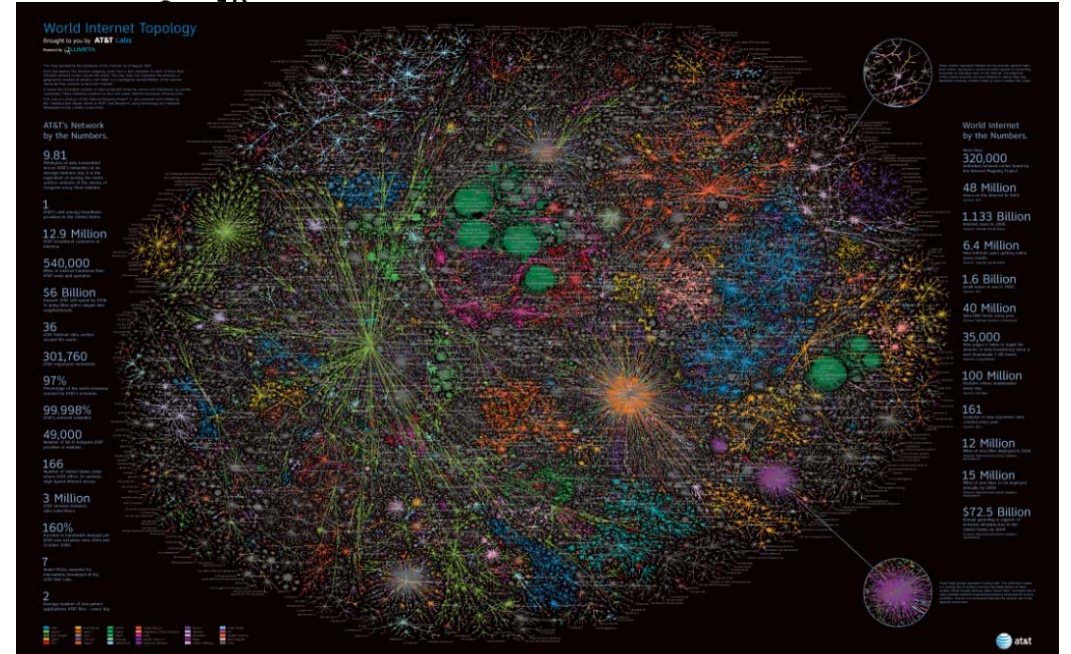
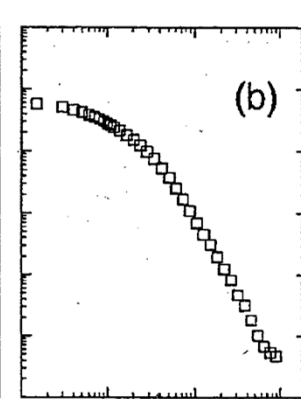
Internet

$$\gamma = 2.4$$



actors

$$\gamma = 2.3$$





Solar flares



Solar flares are high energy explosions from active regions of the sun producing electromagnetic radiation and mass ejections.

Gamma emissions are recorded by telescopes on satellites and accessible in catalogs:

GOES = Geostationary Operational Environmental Satellite for 1.5 – 25 keV

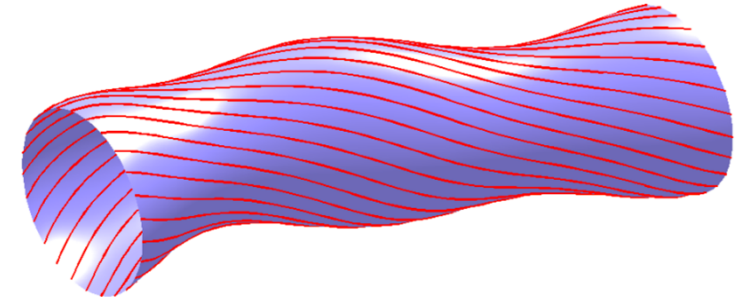
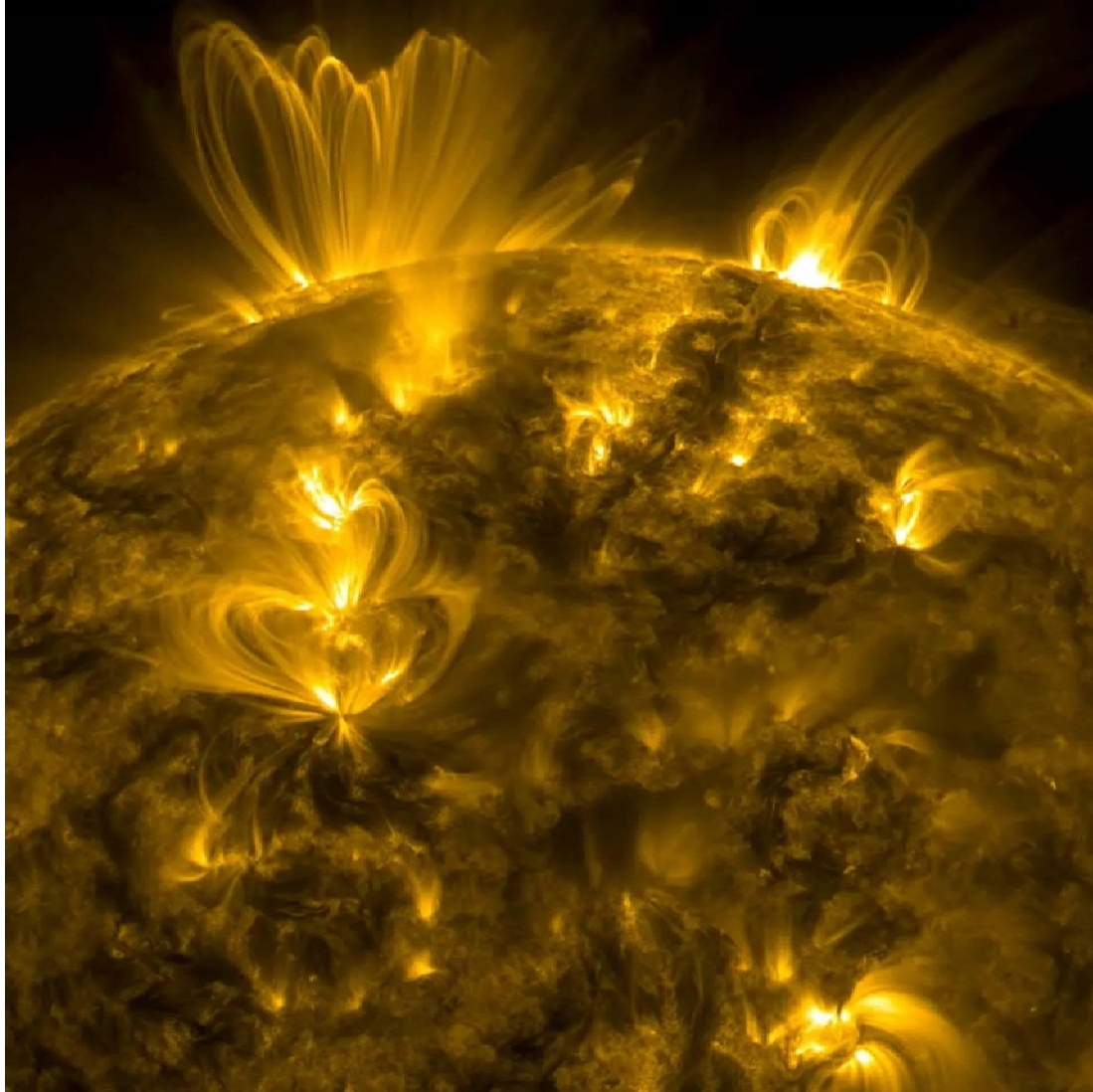
BATSE = Burst and Transient Source Experiment for above 25 keV (till 2000)

WATCH = Wide Angle Telescope for Cosmic Hard X-Rays for 10 – 30 keV (till 1998)



Magnetic flux tubes

Physique et Mécanique
des Milieux Hétérogènes
UMR 7636



The magnetic field lines are wrapped around the flux tubes, forming, when twisted, a spring-shaped bundle.



Magnetic flux tubes



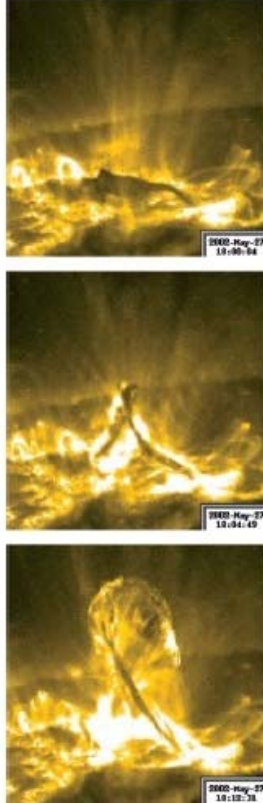


Physique et Mécanique
des Milieux Hétérogènes
UMR 7636



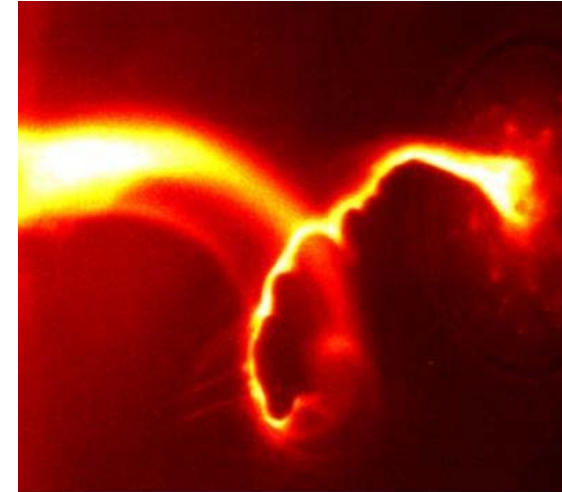
Reconnection





Kink instability

converting
twist into writhe



A kink instability of a flux tube occurs as soon as the intensity of its cumulative twist reaches a given critical value Φ_c .

$\Phi_c \in [2\pi, 12\pi]$ (Srivastava et al, *Astrophys. J.* 715, 292 (2010))

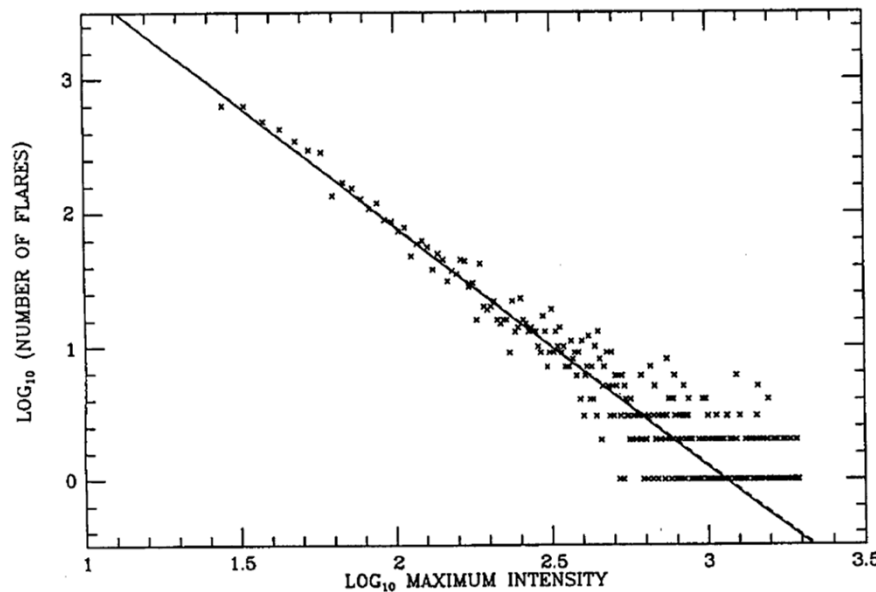
It occurs with the speed of a magnetohydrodynamic wave:
Alfvén speed = $B/\sqrt{\rho\mu} \approx 4400$ km/sec in solar corona

B = magnetic field strength, ρ = fluid density, μ = magnetic permeability



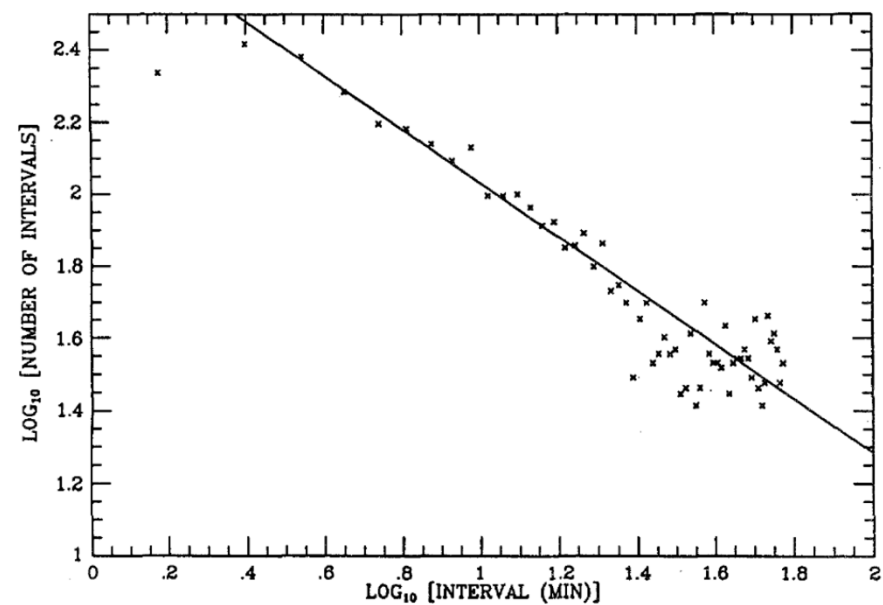
Statistical properties of solar flares

distribution of peak energies E
(peak hard X-ray flux)



$$P(E) \sim E^{-1.8}$$

distribution of intervals Δt
between consecutive events



$$P(\Delta t) \sim \Delta t^{-0.75}$$

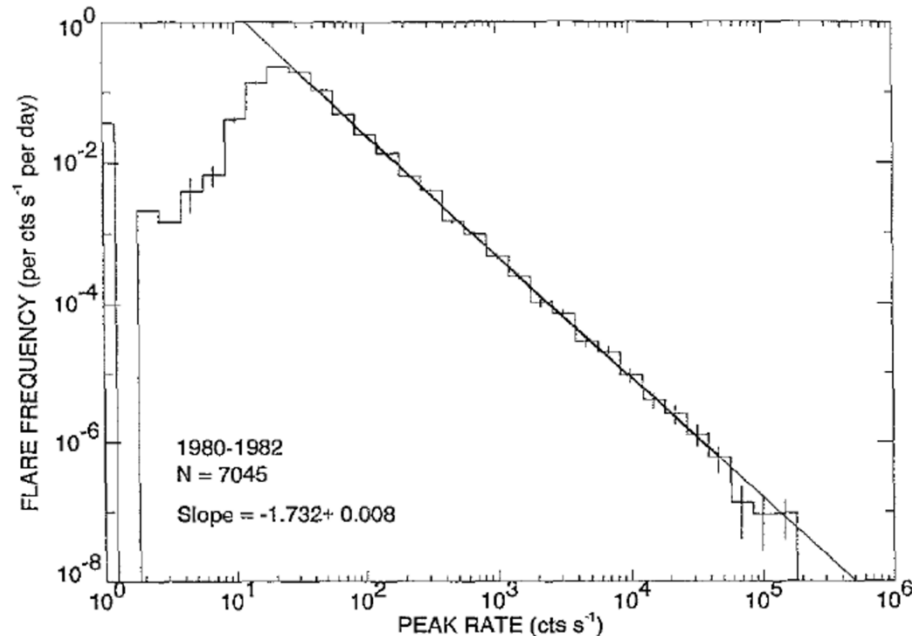
Hard X-Ray Burst Spectrometer (HXRBS), 1980-1989

Pearce et al, *Astrophys. Space Sci.* 208, 99 (1993)

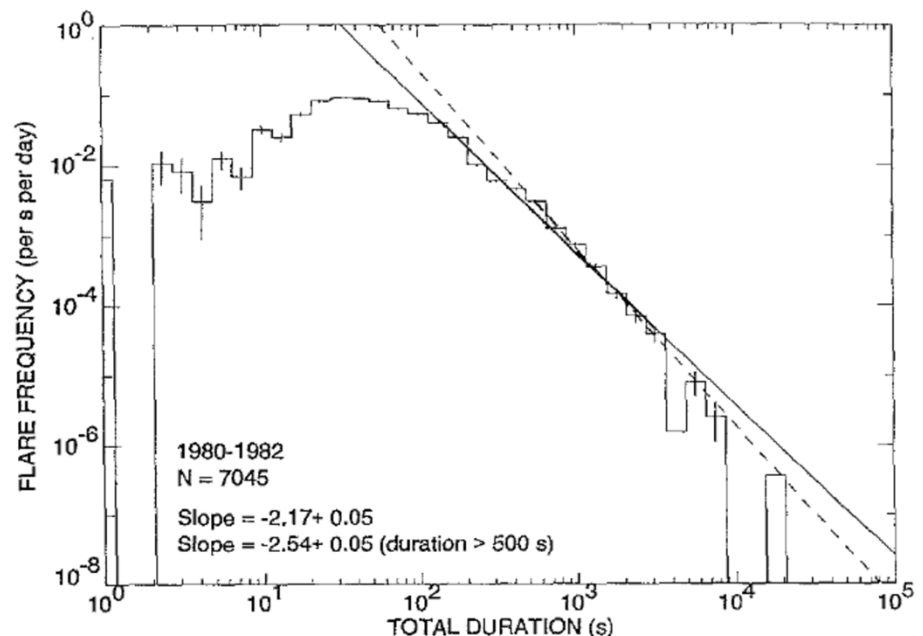


Statistical properties of solar flares

distribution of peak rates n



distribution of flare durations τ



$$P(n) \sim n^{-1.73}$$

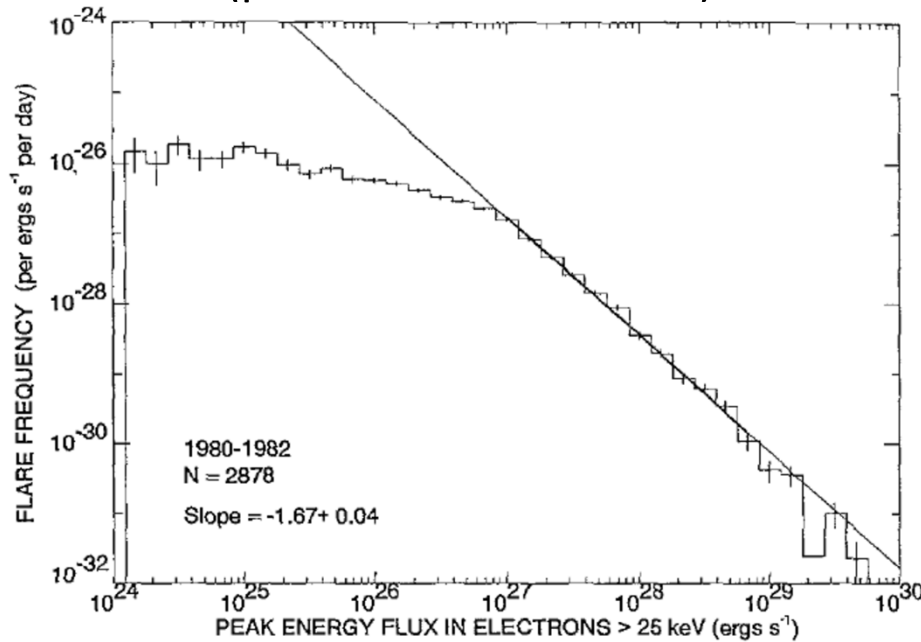
$$P(\tau) \sim \tau^{-2.17}$$

Hard X-Ray Burst Spectrometer (HXRBS), 1980-1982

Crosby, Aschwanden & Dennis, Solar Phys. 143, 275 (1993)

Statistical properties of solar flares

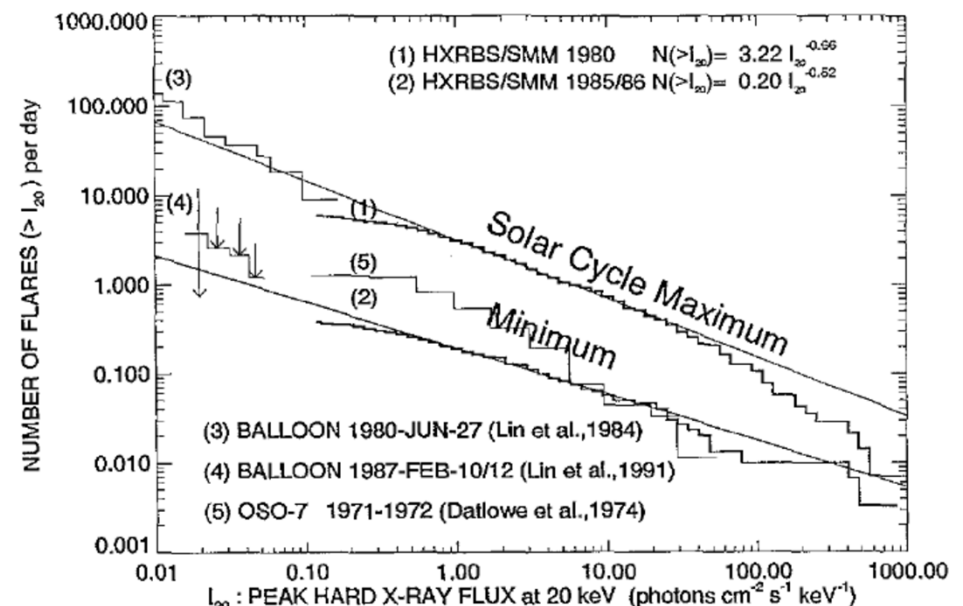
distribution of peak energies E
(peak flux in electrons)



$$P(E) \sim E^{-1.53}$$

Hard X-Ray Burst Spectrometer (HXRBS), 1980-1982

dependence on the solar cycle

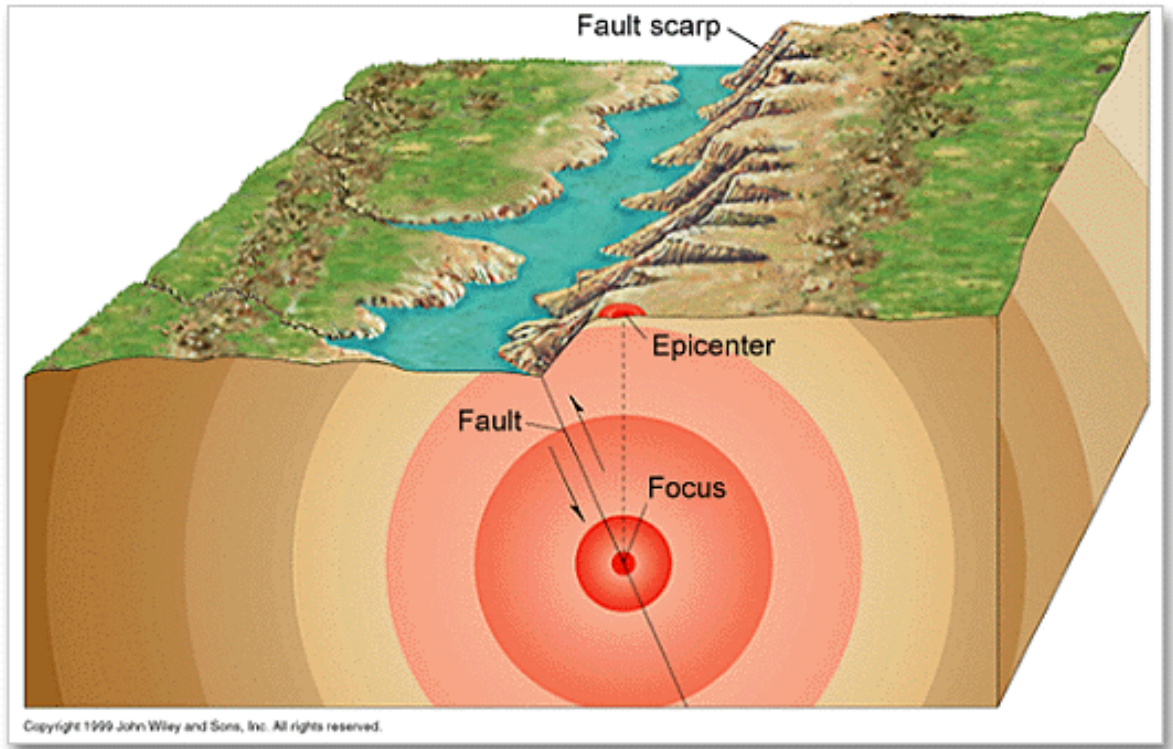
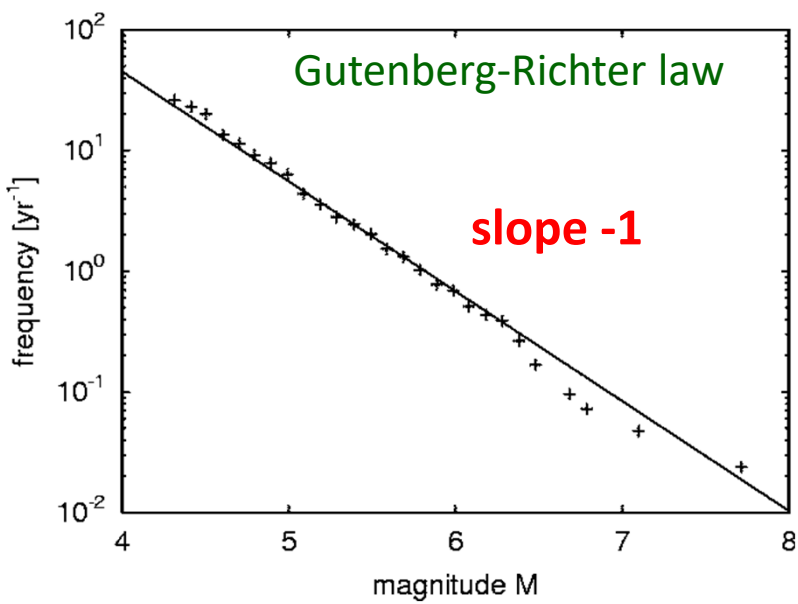
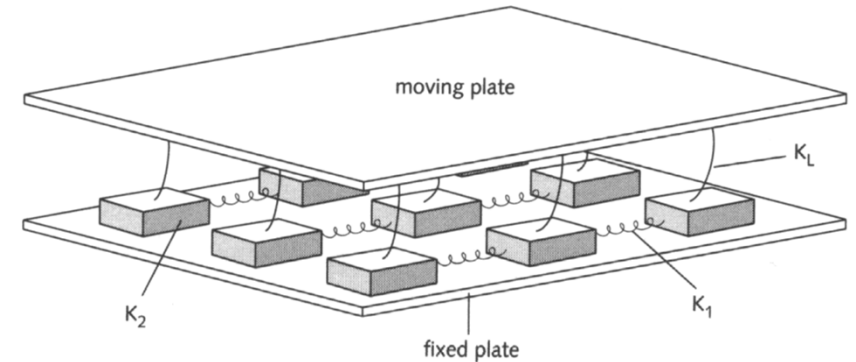


Crosby, Aschwanden & Dennis, Solar Phys. 143, 275 (1993)



Earthquakes

Physique et Mécanique
des Milieux Hétérogènes
UMR 7636



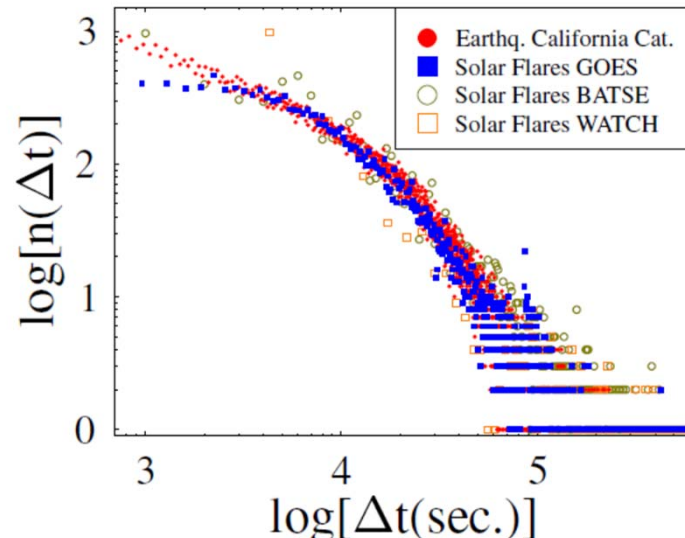


Similarity with earthquakes

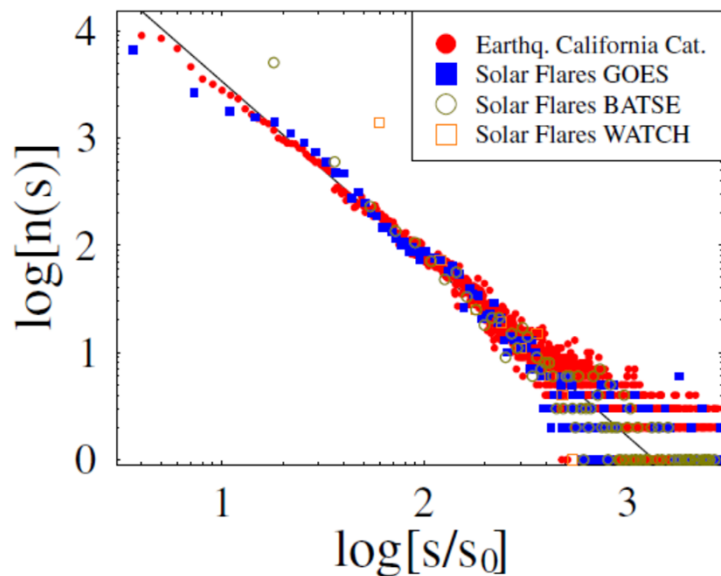
Physique et Mécanique
des Milieux Hétérogènes
UMR 7636



waiting time distributions

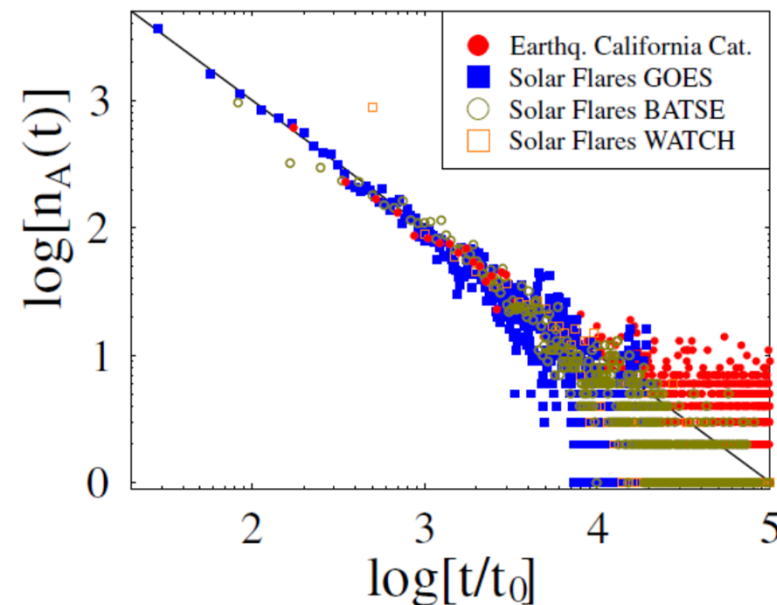


distributions of peak intensities



Omori law

distributions of number of events a time t
after a main event



L. de Arcangelis, C. Godano, E. Lippiello &
Nicodemi, Universality in solar flare and
earthquake occurrence. Phys. Rev. Lett. 96,
051102 (2006)



SOC model for solar flares

Magnetic field vector B_i on each site of a cubic lattice. If local gradient:

$$dB_i = B_i - (1/6) \sum_{nn} B_{nn}$$

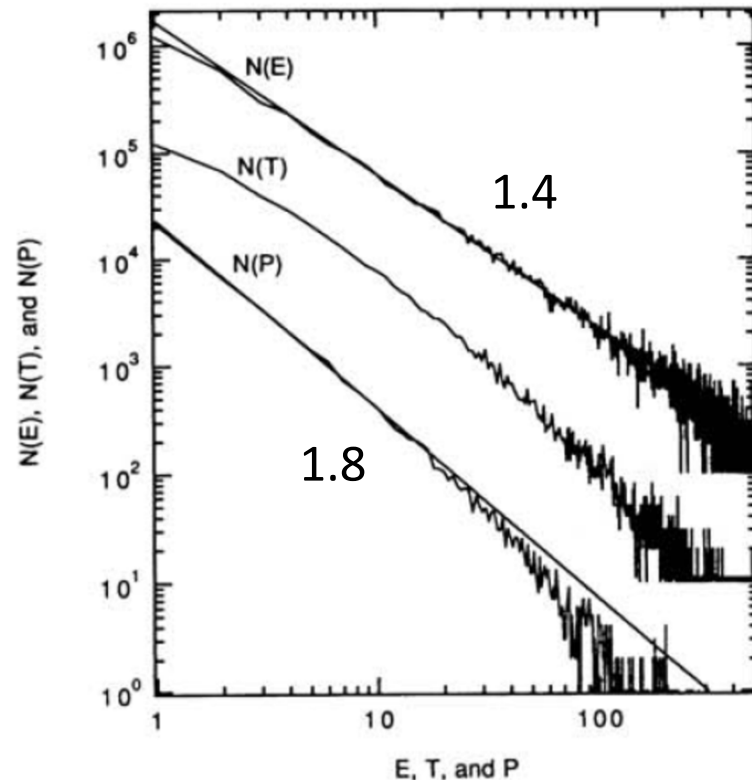
exceeds a certain threshold B_c

$$|dB_i| > B_c$$

the field is distributed to the neighbors

$$B_i \rightarrow B_i - (6/7) dB_i \quad \text{and} \quad B_{nn} \rightarrow B_{nn} + (1/7) dB_i$$

→ avalanche dynamics



Energy, flux and duration of avalanches are power-laws

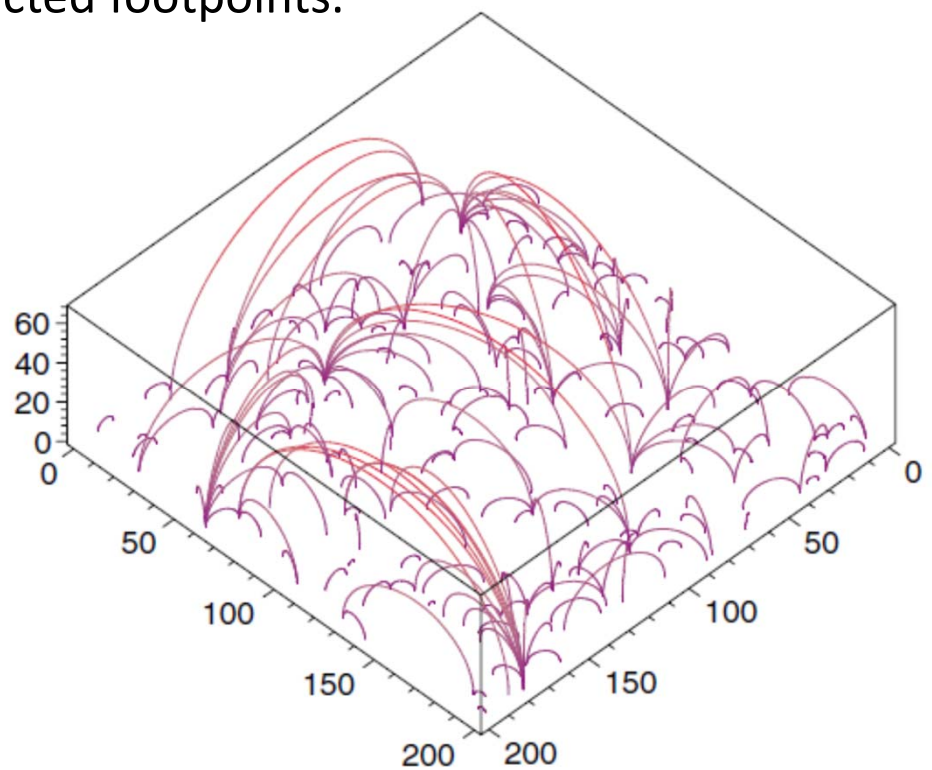
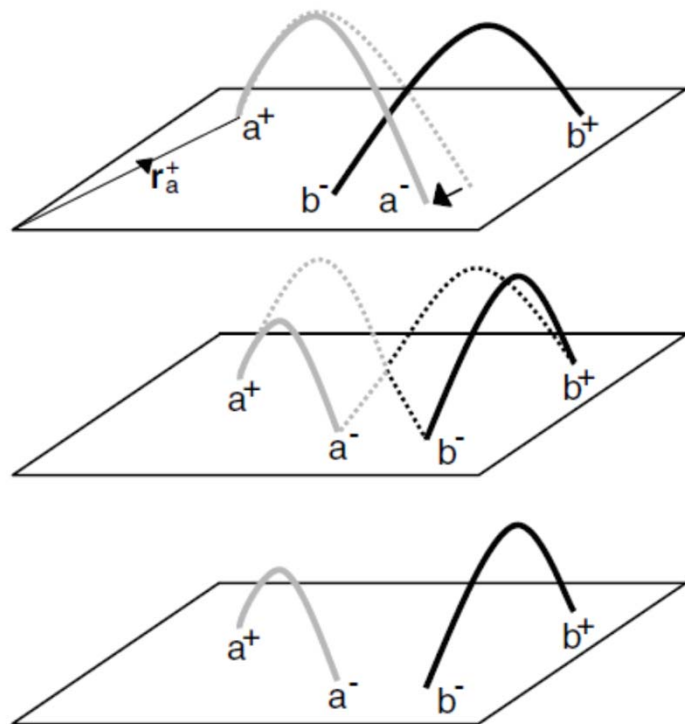
but distribution of waiting times is Poissonian.

E. Lu, and R.J. Hamilton, *Astrophys. J.*, 380, L89 (1991)



SOC model for solar flares

Directed magnetic loops going from a positive to a negative footpoint are injected at random positions. The footpoints perform random walks. Reconnection occurs when two loops cross or when footpoints of opposite polarity annihilate. While reconnecting other loops might be crossed generating avalanches of reconnections. When footpoints of same polarity come close they can merge creating multiply connected footpoints.

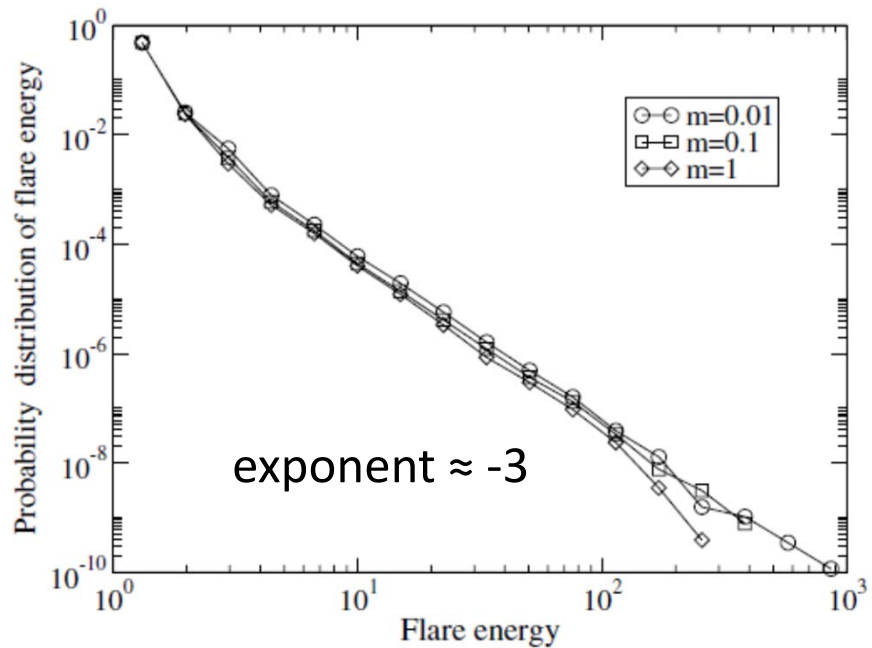


Hughes, D., Paczuski, M., Dendy, R. O., Helander, P. & McClements, K. G. Solar flares as cascades of reconnecting magnetic loops. Phys. Rev. Lett. 90, 131101 (2003)



Results

distribution of flare energies

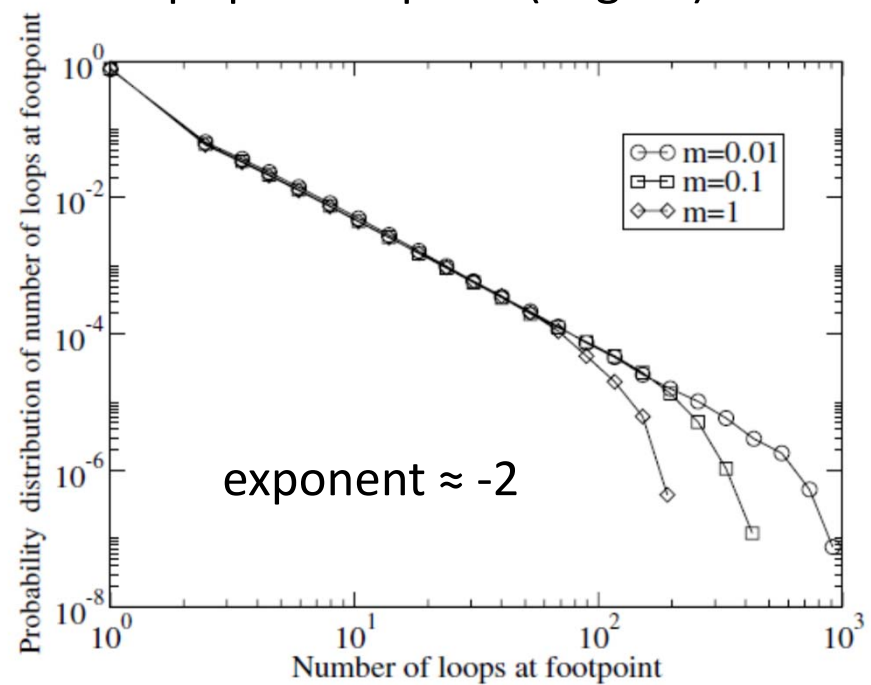


energy is equal to the length of the loop:

$$E = (\pi/2) | \mathbf{r}_+ - \mathbf{r}_- |$$

distribution of individual loop lengths
is however exponential

distribution of the number of loops per footpoint (degree)



→ scale-free network

but distribution of waiting times
is Poissonian



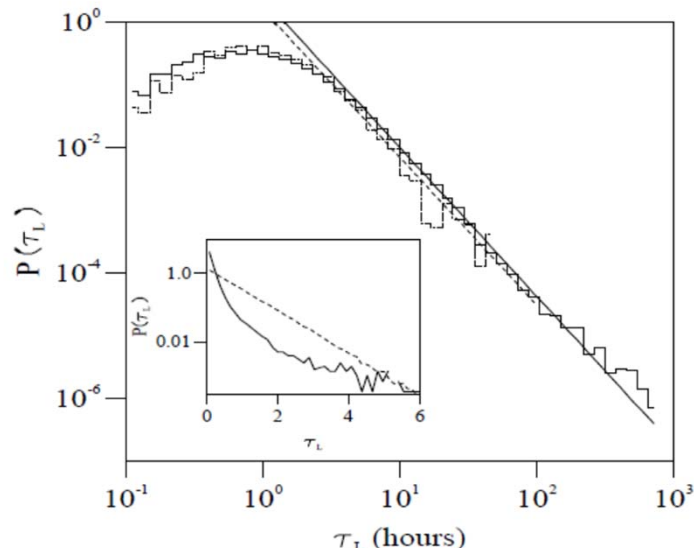
SOC vs turbulence

Power Laws in Solar Flares: Self-Organized Criticality or Turbulence? G. Boffetta , V. Carbone, P. Giuliani, P. Veltri and A. Vulpiani, Phys. Rev. Lett. 83, 4662 (1999)

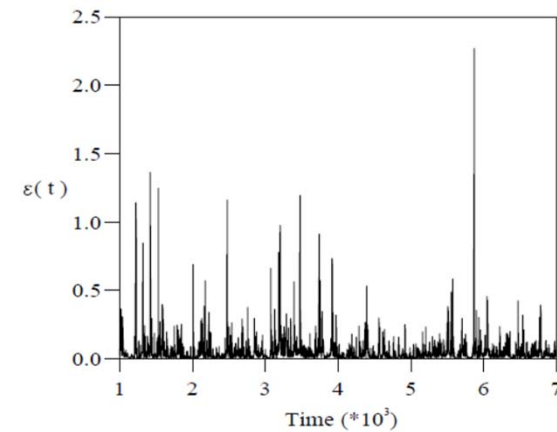
shell model for MHD

u_n and b_n are scalar velocity and magnetic field at wavenumber $k_0 2^n$.
coupled system of quadratic equations
→ simple dynamical system

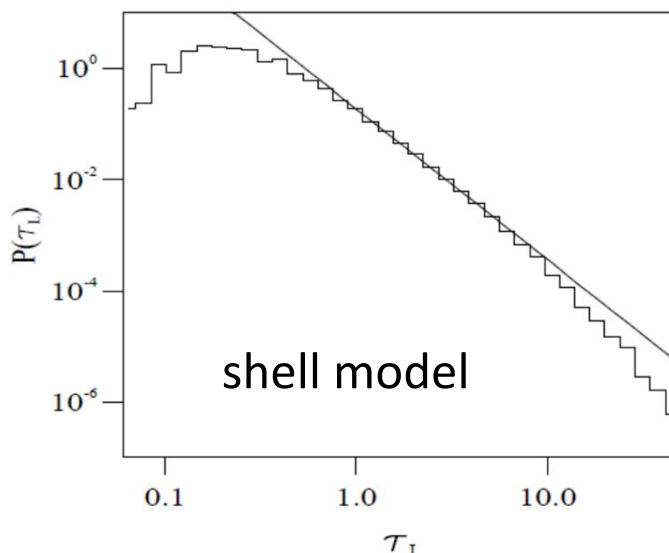
distribution of waiting times:



HXR bursts associated to flares (1976 – 1996)



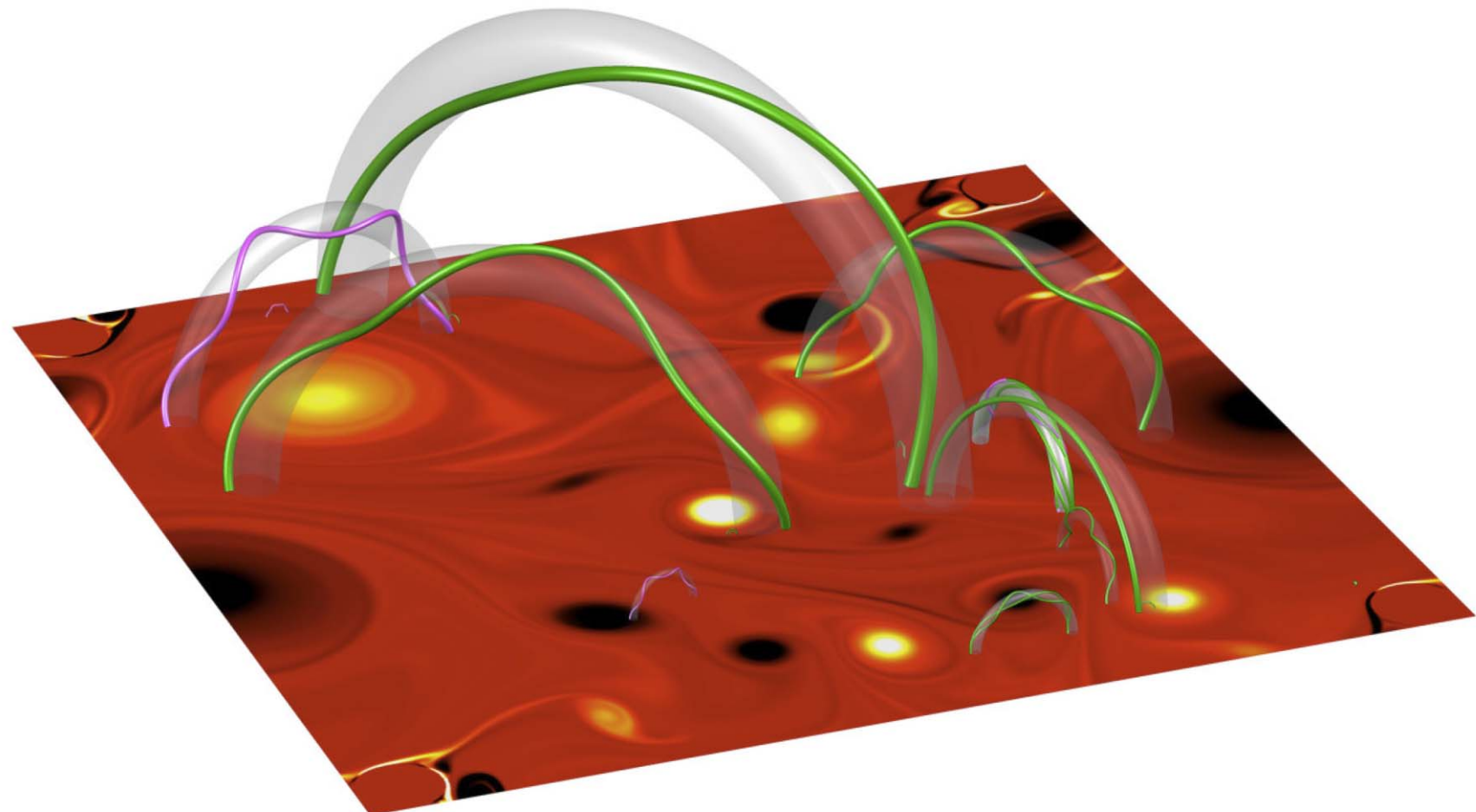
intermittent
time evolution of
energy dissipation
in shell model



but exponents depend on threshold



Simulation of solar flares



M. Mendoza, A. Kaydul, L. De Arcangelis, J.S. Andrade Jr., H.J.H.
Modelling the influence of photospheric turbulence on solar flare statistics
Nature Comm. 5, 5035 (2014)



Collaborators



Miller Mendoza



Alan Kaydul



Lucilla de Arcangelis



José Soares Andrade Jr.



The Model

Reconnection of magnetic flux tubes occurs due to kink instabilities. The footpoints follow the local velocity field of the turbulent flow of the photosphere and are therefore **twisted**.

Positions of footpoints:

$$\mathbf{x}_{l\pm}(t + \delta t) = \mathbf{x}_{l\pm}(t) + \mathbf{u}(\mathbf{x}_{l\pm})\delta t$$

where $\mathbf{u}(\mathbf{x})$ is the local velocity of the fluid at position \mathbf{x} .

Cummulative twist w_{l+} and w_{l-} :

$$w_{l\pm}(t + \delta t) = w_{l\pm}(t) + (\nabla \times \mathbf{u})_z \delta t$$

The photosphere is considered two-dimensional since its thickness (≈ 500 km) is much smaller than the radius of the sun.



The Model

Interaction between reconnection events:

After a reconnection event we multiply the cumulative twist of neighbouring tubes by a factor λ .

If $\lambda > 1$, this means that the reconnection heats up the surrounding plasma increasing the local pressure, and therefore, increasing the critical twist Φ_c of the surrounding magnetic flux tubes.

If $\lambda < 1$, this means that the twist of the surrounding tubes is increased, triggering new flares and generating a cascade of events → avalanches.

$\lambda = 1$ means no interaction between tubes.

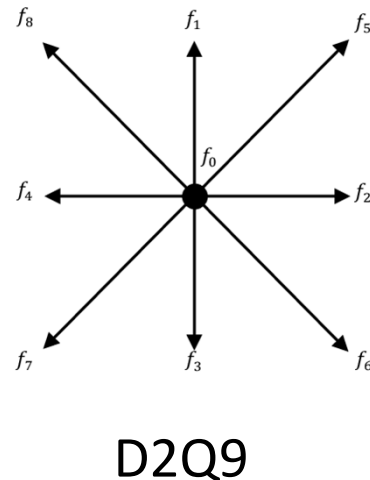


Simulation of 2d turbulence using LBM

“Two-dimensional turbulence with the lattice Boltzmann equation”

R Benzi and S Succi, J. Phys. A: Math. Gen. 23 L1 (1990)

discrete velocities



We consider a square lattice of size $L \times L$.

Lattice Boltzmann equations (BGK):

$$f_i(x + v_i, v_i, t + 1) - f_i(x, v_i, t) + F_i(v_i) = \frac{1}{\tau} [f_i^0(\rho_n, u, T) - f_i(x, v_i, t)]$$

$$f_i^0 = \rho_n w_i \left[1 + \frac{3\vec{v}\vec{u}}{c_s^2} + \frac{9(\vec{v}\vec{u})^2}{2c_s^4} - \frac{3\vec{u}^2}{2c_s^2} \right]$$

forcing term:

$$Re = 10^4 - 10^5$$

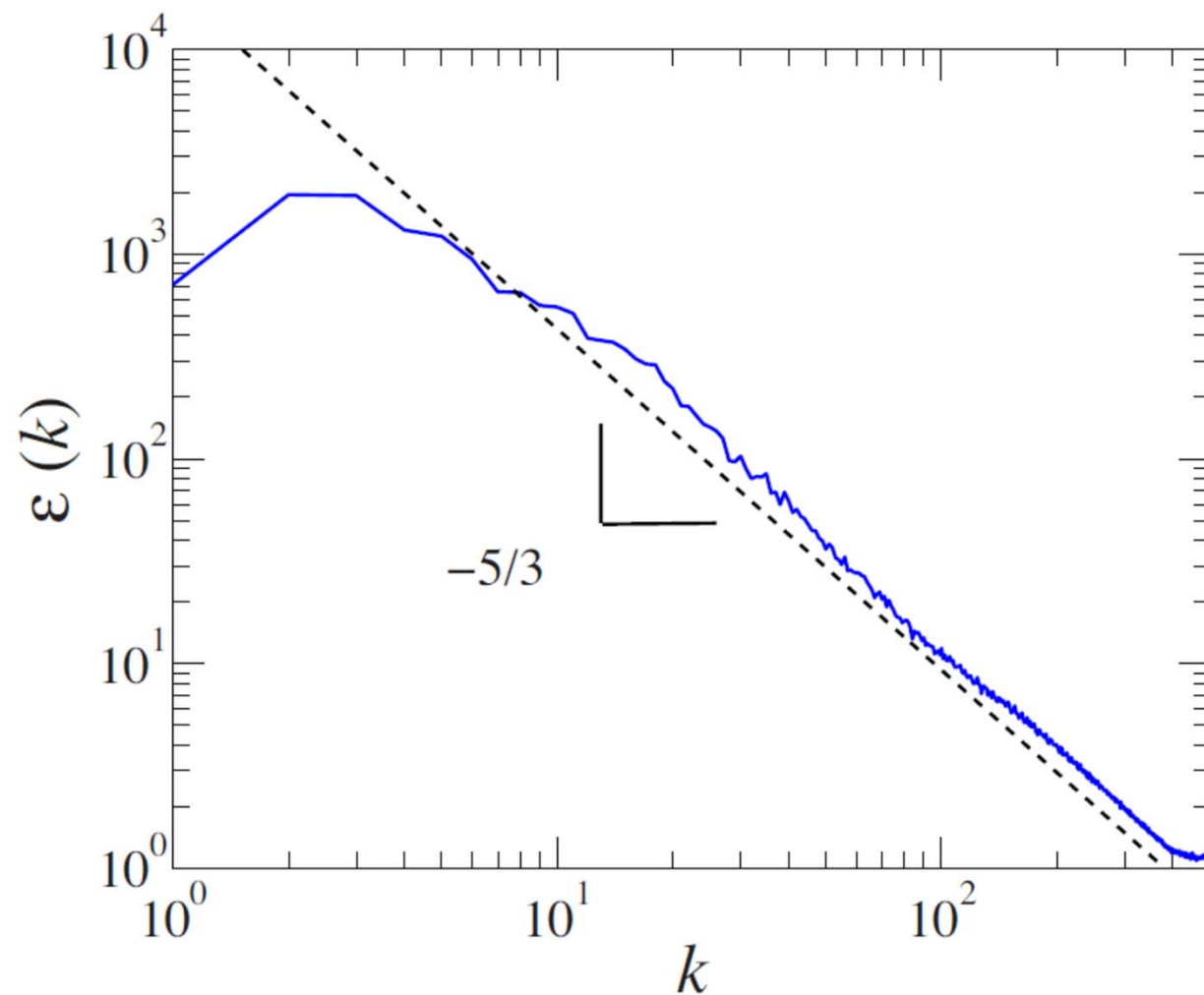
$$\mathbf{F} = A_0 (\sin(k_f x) \cos(k_f y), -\cos(k_f x) \sin(k_f y))$$

$$\nabla \cdot \mathbf{F} = 0 \quad A_0 = 10^{-8}$$

Simulated on a cluster of 12 graphic cards, Nvidia Tesla M2075, each with 448 GPU cores.



Energy spectrum of photospheric turbulence



$L = 2048$

→ Kolmogorov



The Model

Once the turbulent velocity field exhibits Kolmogoroff scaling we add at random positions N magnetic flux tubes having an outer radius $R = 4$ and zero twist at their footpoints.

Since the position of footpoints is, in general, not located at a fluid grid point, we use bilinear interpolation to calculate the velocity at the footpoint position.

The energy of a tube is given by the length of the magnetic line, which depends on the twisting and the size of the semi-circular tube:

$$E_l = \int_0^\pi \sqrt{\frac{d\mathbf{R}_l}{d\omega} \cdot \frac{d\mathbf{R}_l}{d\omega}} d\omega$$

with

$$\mathbf{R}_l(\omega) = (([R + r_c] + r_c \cos(\omega)) \cos(\xi), r_c \sin(\omega), ([R + r_c] + r_c \cos(\omega)) \sin(\xi))$$

where r_c is the cross-section radius of the semi-circular tube and $\xi = \Theta\omega$
where $\Theta = w_{l+} + w_{l-}$ is the number of turns.



The Model

Once the twist $\Phi = \pi R \Theta / (2r_c + R)$ of a magnetic flux tube reaches the critical twist Φ_c , the tube releases its entire energy and vanishes. Then a small new tube is inserted at a random position.

Our model neglects:

- stratified 3d structure of Sun's surface
- interaction between flow and magnetic field
- other reconnection mechanisms
- slip-running magnetic reconnection in flares
- intense magnetic polarity inversion lines in the photosphere
- peculiar flows on top of the quiet-Sun flow velocity field
-
-



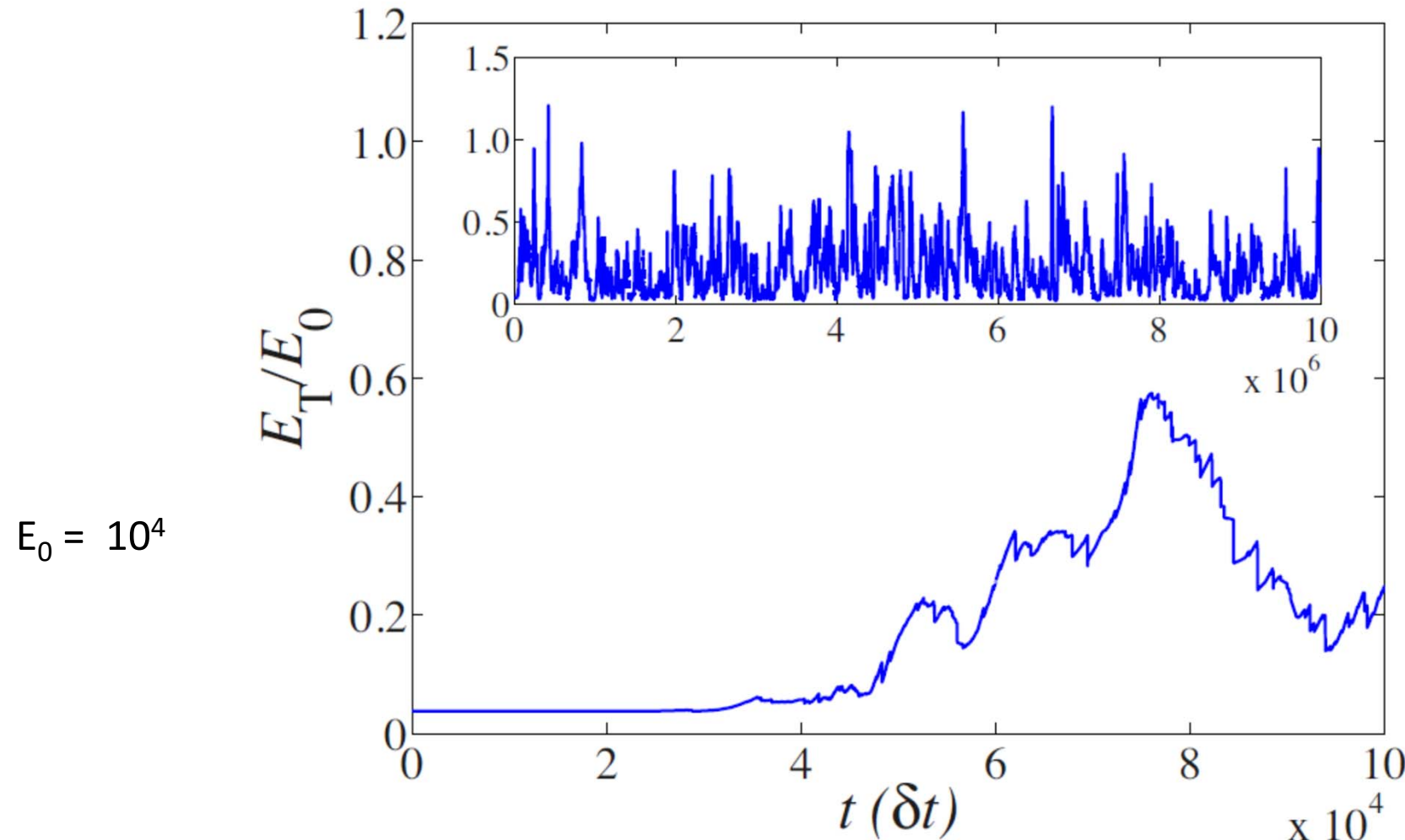
Simulation parameters for different sizes

L	Re	N	N_e
128	9×10^3	100	200000
256	1.7×10^4	200	200000
512	3.5×10^4	400	200000
1024	6.0×10^4	800	175100
2048	1.1×10^5	1600	150000



temporal evolution of total energy E_T

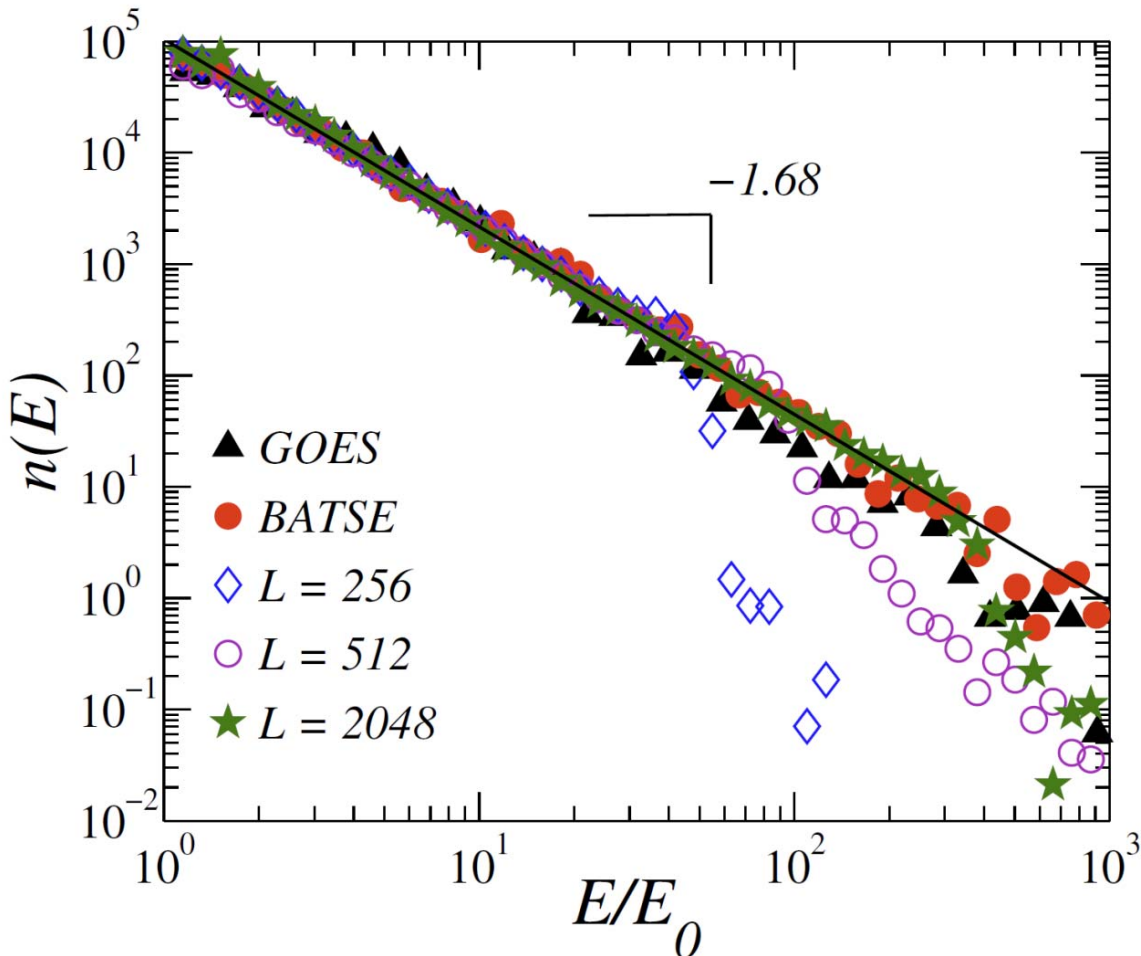
E_T is the sum of the magnetic energy of all loops at a given time.



$$L = 512, N = 100, r_c/R = 0.1, \lambda < 1, \Phi_c = 4\pi$$



Distribution of peak energies



GOES 19703 events 1992 – 2013, $E_0 = 10^{-6} \text{ Wm}^{-2}$
BATSE 7242 events 1991 – 2000, $E_0 = 0.5 \text{ counts s}^{-1} \text{ cm}^{-2}$

Kolmogorov–Smirnov test:

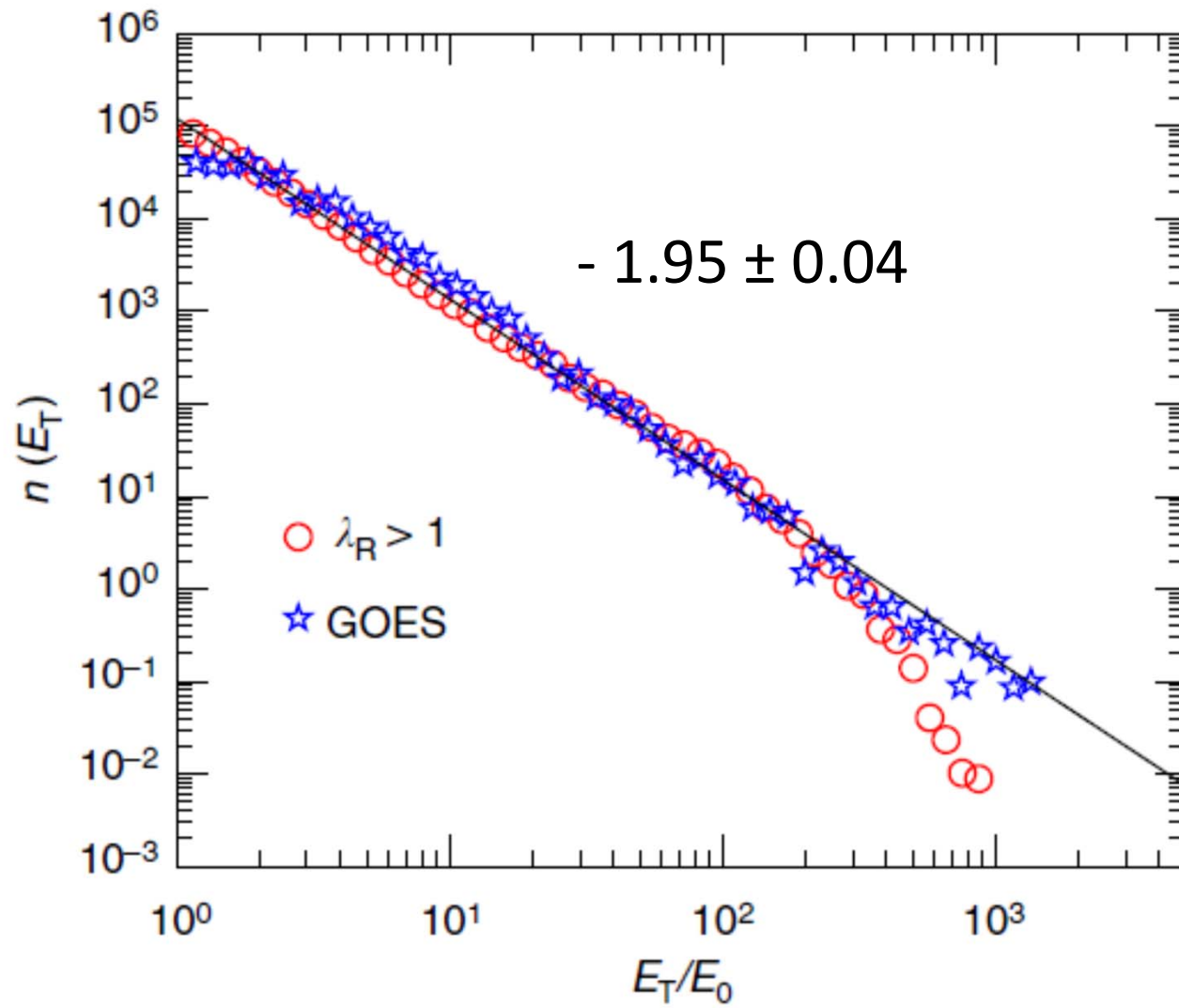
P value of 95%
(confidence level of 99%)

$\lambda < 1$
(no avalanches)

numerical data: $E_0 = 10$



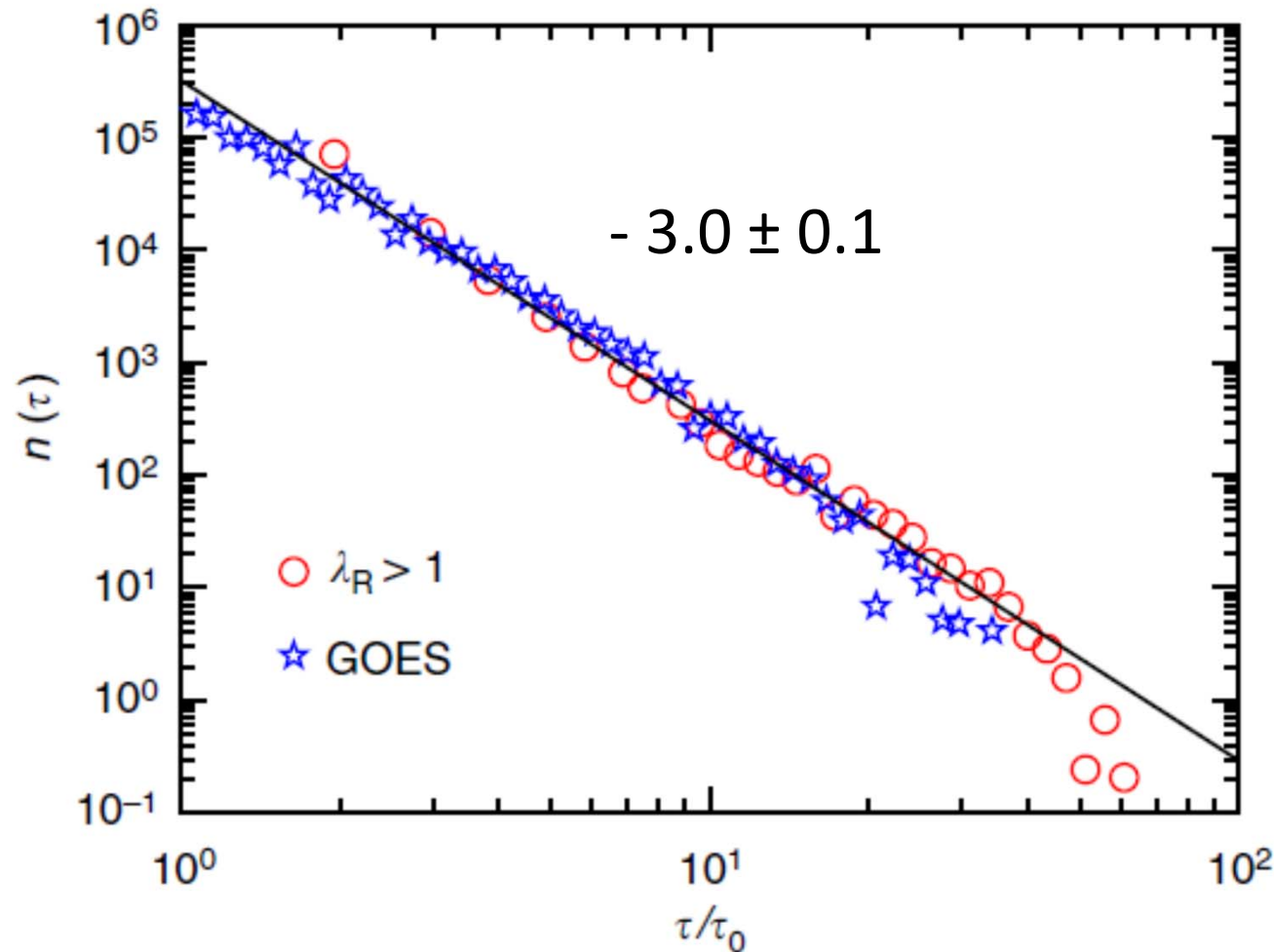
Distribution of total energies



$L = 512, N = 400, \lambda > 1$



Distribution of flare durations



GOES: $\tau_0 = 10^3$ s

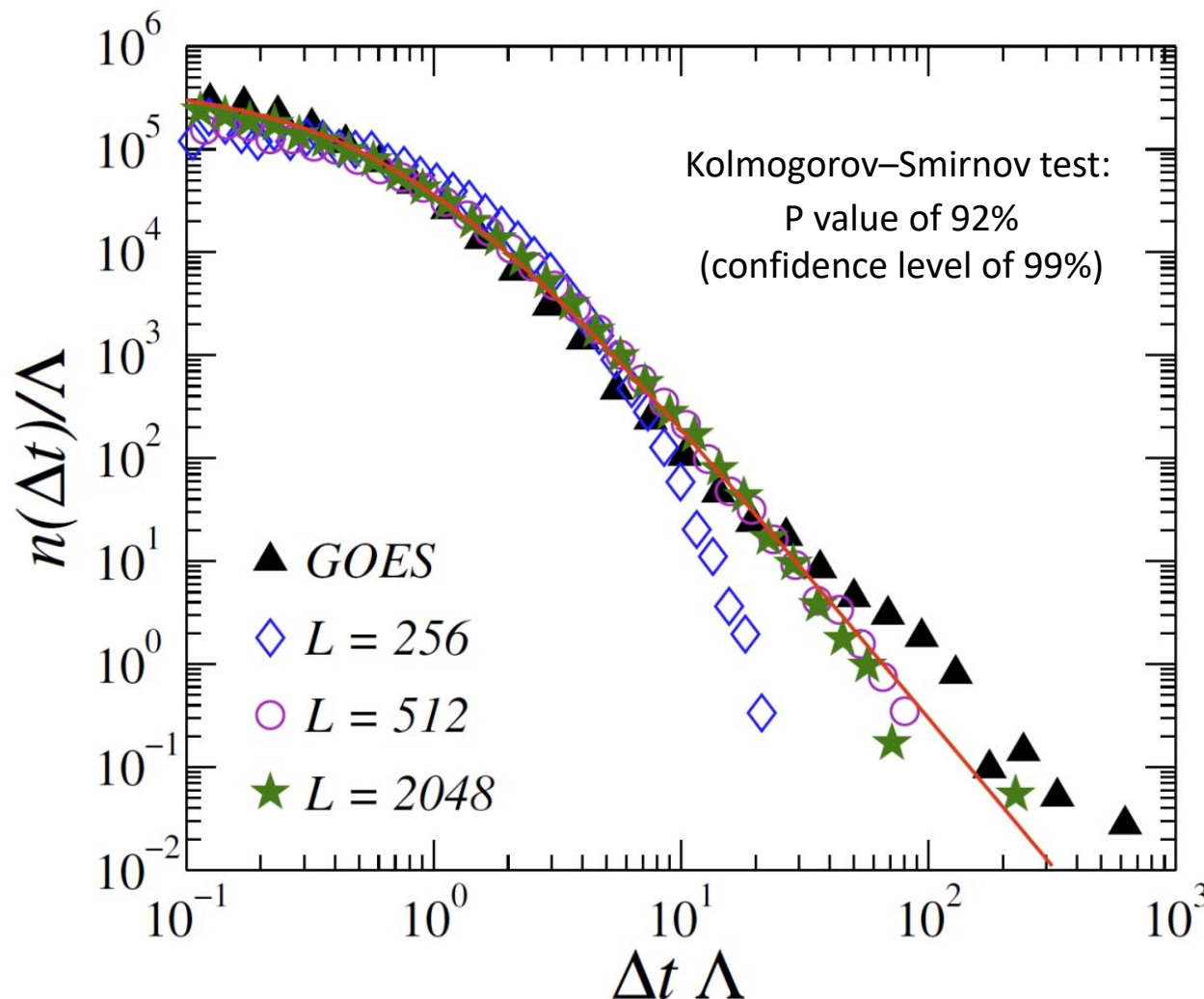
numerical data: $\tau_0 = 1$



Distribution of waiting times

inverse average waiting time: $\Lambda = N_e / (t_{\max} - t_{\min})$

N_e = number of events in the catalogue



we find

$$n(\Delta t)/\Lambda = a/(1 + b\Delta t\Lambda)^\alpha$$

with

$$\alpha = 2.8 \pm 0.2$$

Wheatland, 2000:

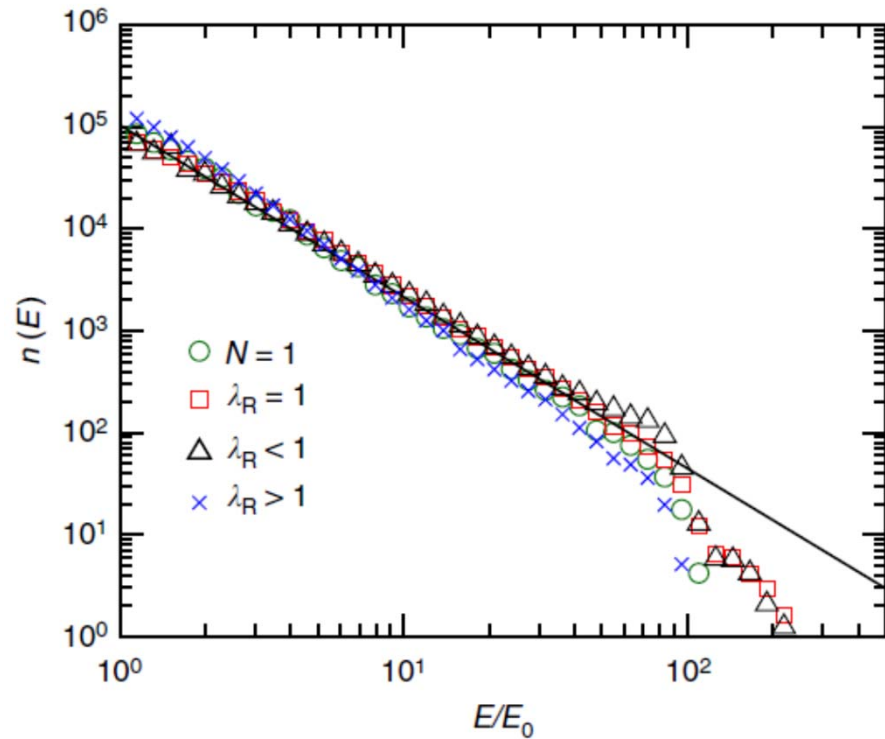
$$\alpha = 2.12 \pm 0.05$$

Boffetta et al, 1999:

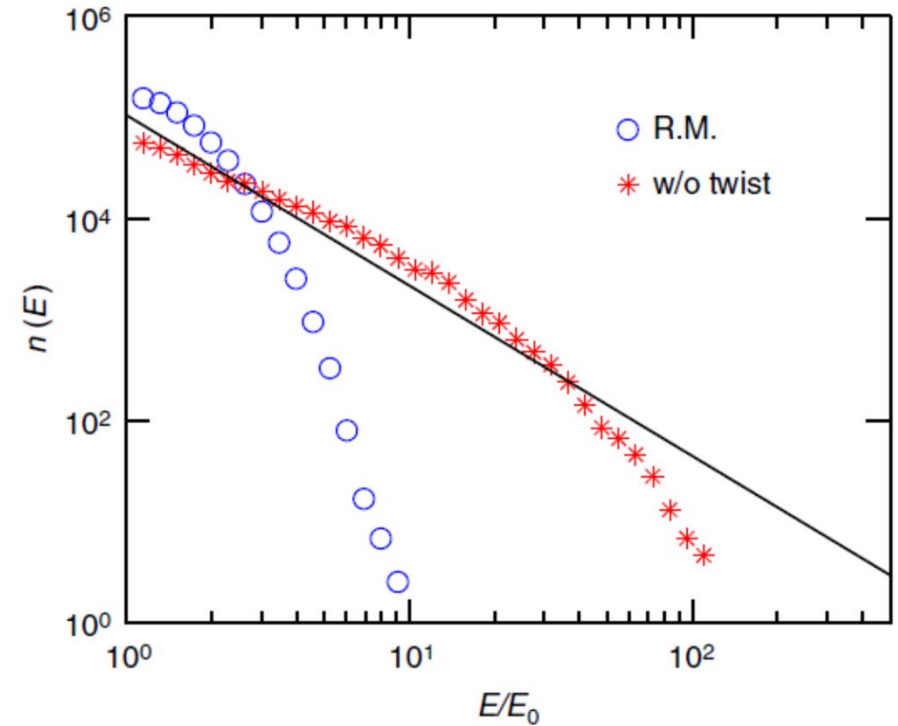
$$\alpha = 2.4 \pm 0.1$$



Distribution of peak energies



$L = 512$

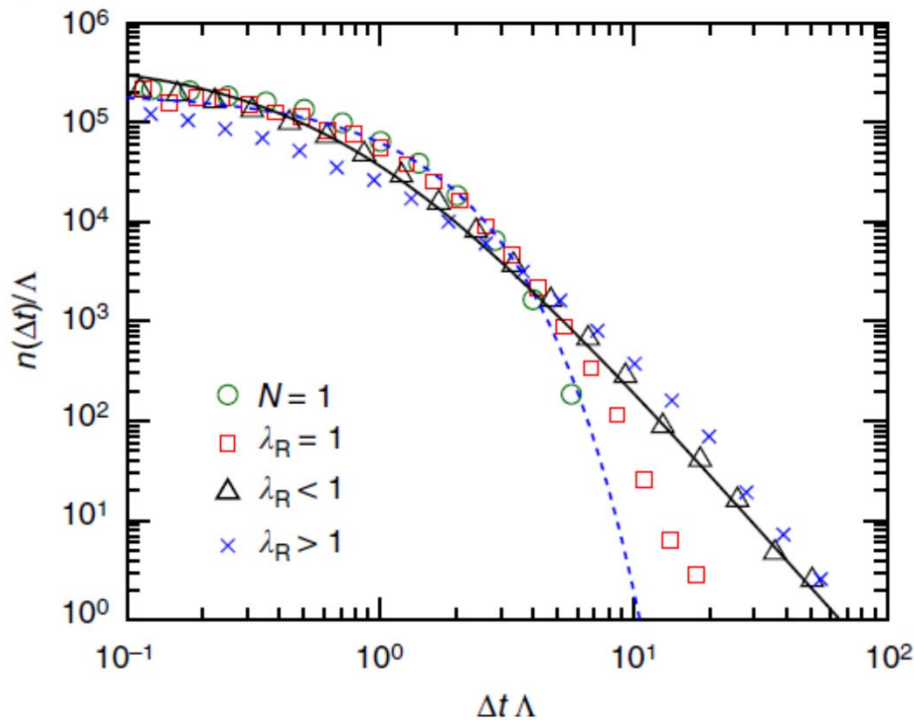


$N = 400, \lambda < 1$

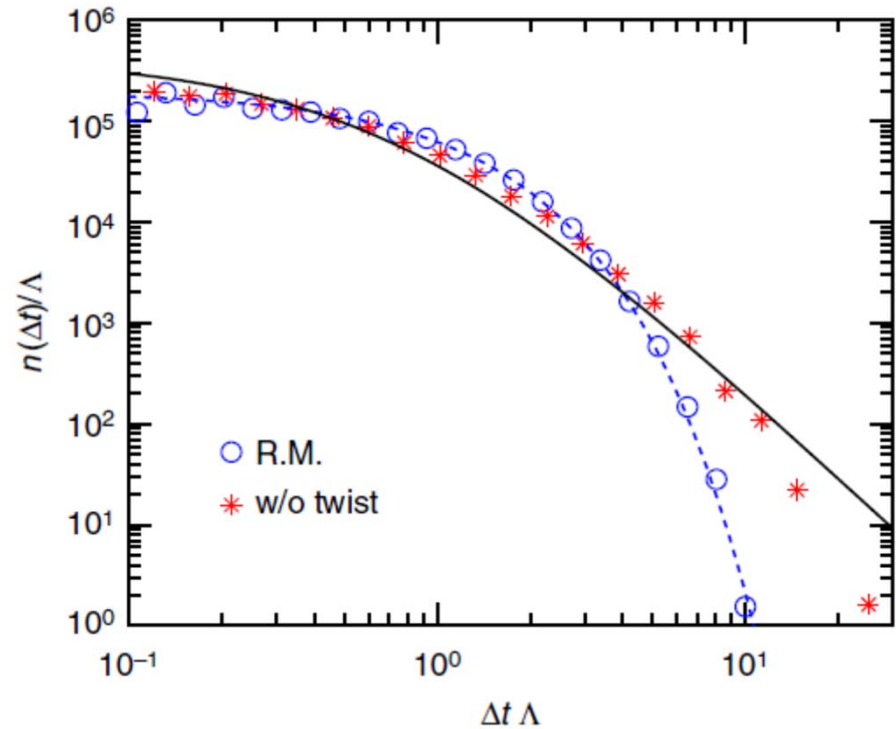
R.M. = footpoints perform random walk



Distribution of waiting times



$L = 512$



R.M.= footpoints perform random walk

$N = 400, \lambda < 1$



Correlation between energies and occurrence times

probability that a flare of energy E_i is followed by a flare of energy λE_i under the condition that their temporal distance Δt is smaller than t_{th} :

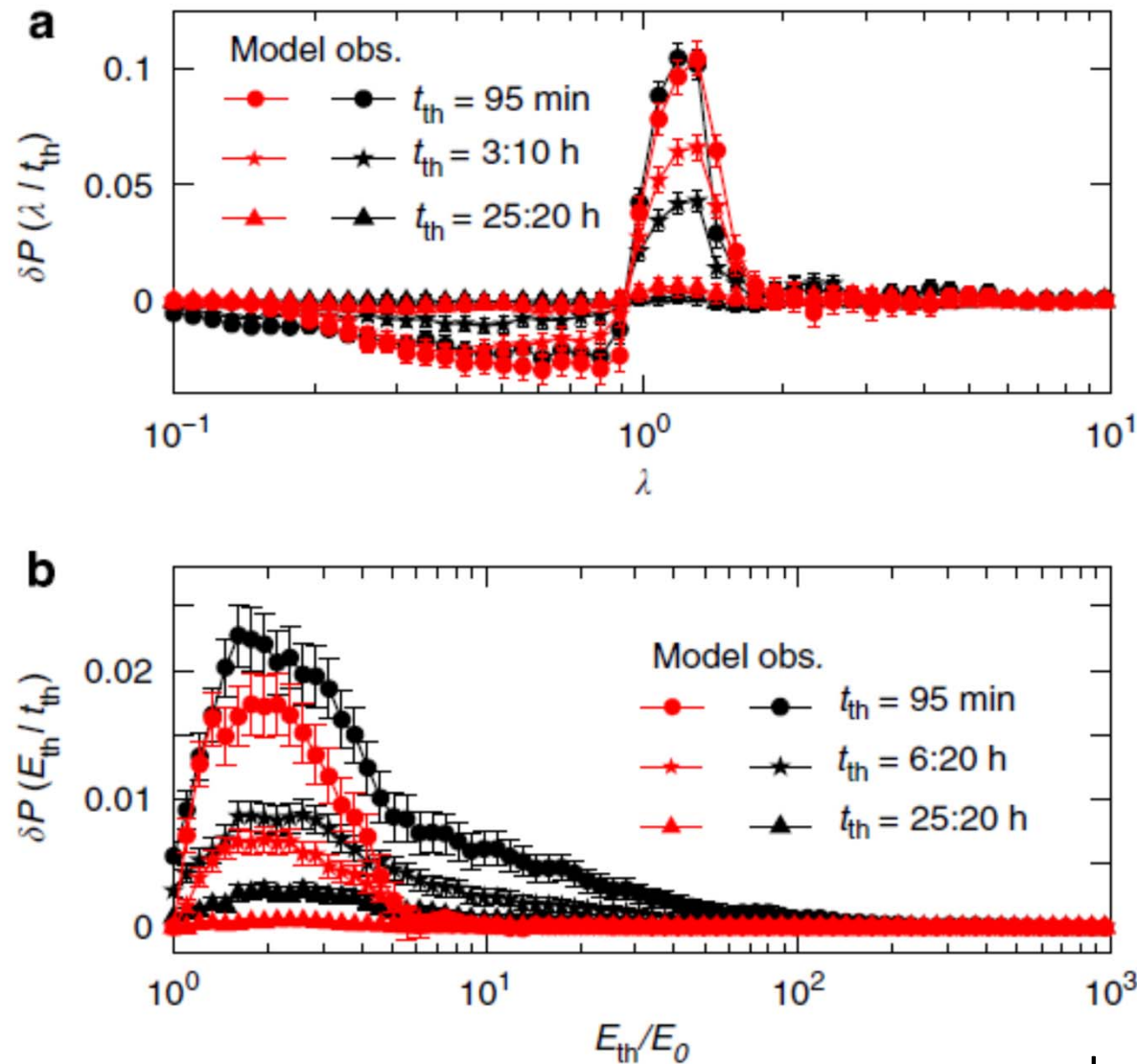
$$P(\lambda|t_{th}) = P(E_{i+1}/E_i > \lambda | \Delta t_i < t_{th})$$

$$\delta P(\lambda|t_{th}) = P(\lambda|t_{th}) - P(\lambda|t_{th})$$

original time series

randomly reshuffled time series
averaged over 10^5 reshufflings

Correlation between energies and occurrence times



For consecutive flares occurring within 3 h, the energy of the second flare is larger than the energy of the previous one.

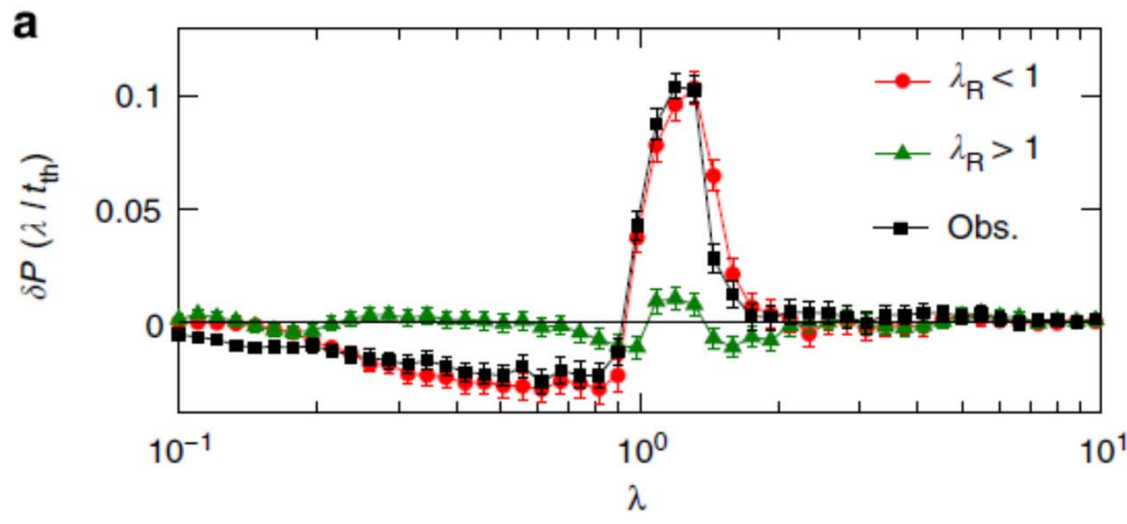
As consecutive flares become more distant in time, the probability to find the following flare with energy higher than E_{th} becomes smaller for $E_{\text{th}} < 10 E_0$.

numerical data: $E_0 = 150$

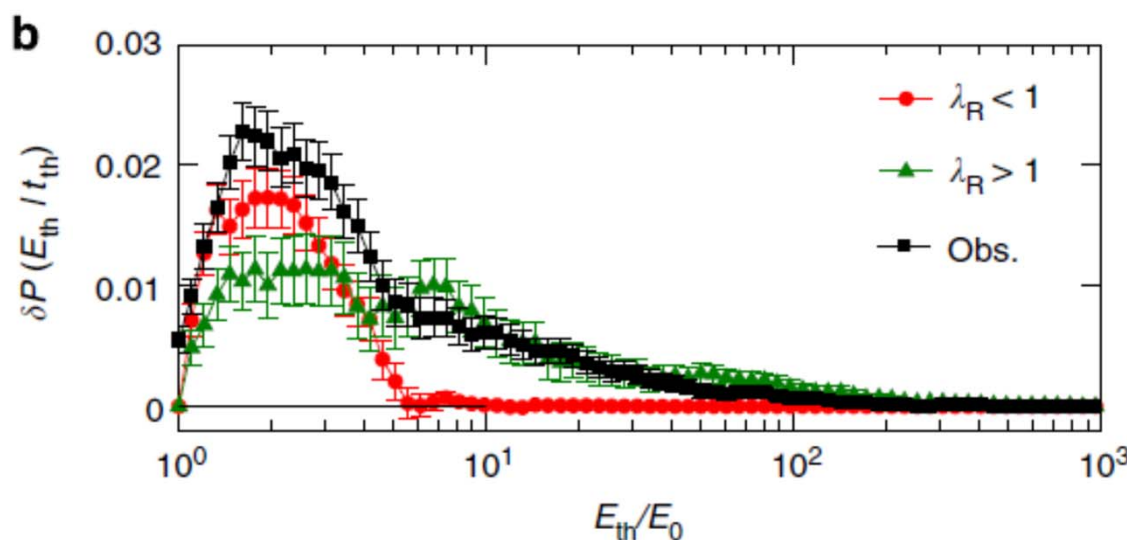
observational data: $E_0 = 1.5 \cdot 10^{-6} \text{ Wm}^{-2}$



Correlation between energies and occurrence times

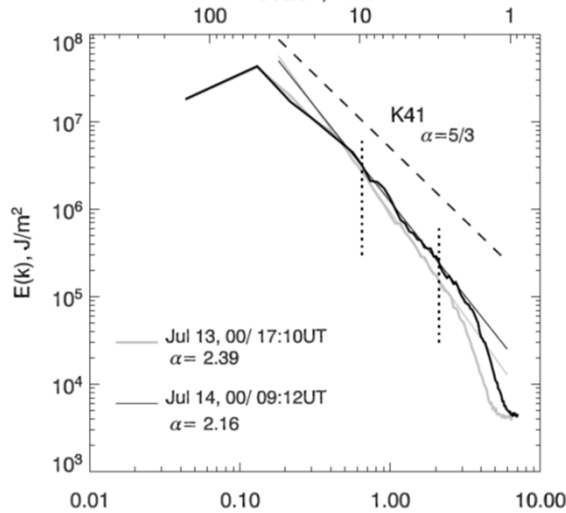


$t_{th} = 95$ min





Kolmogoroff spectrum

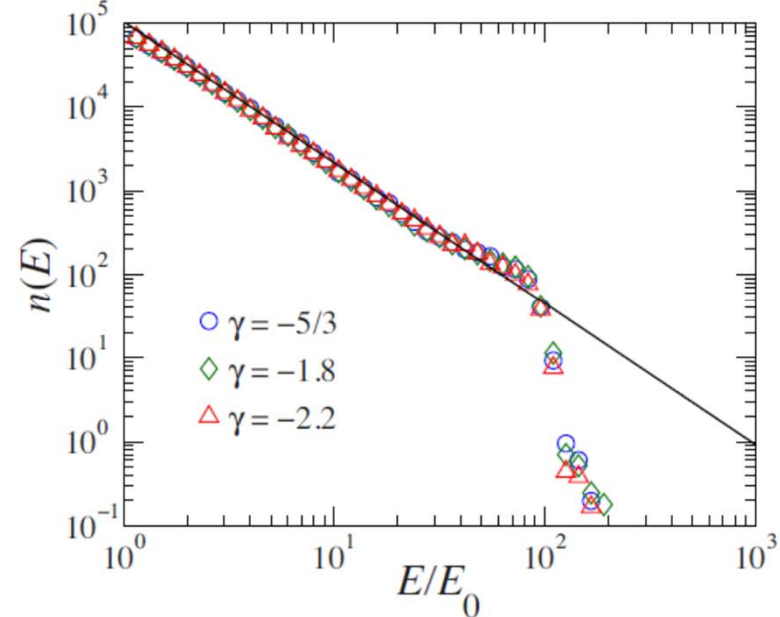
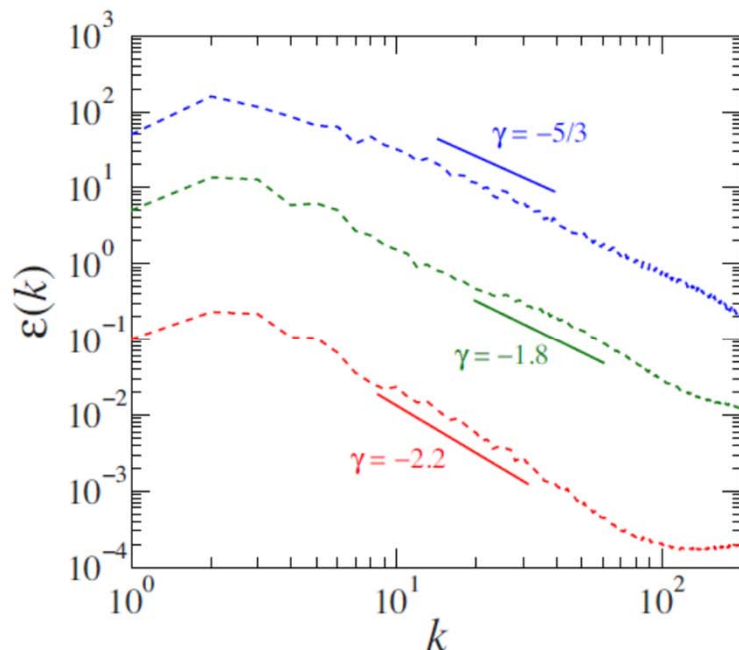


power spectra from active region
(Solar and Heliospheric Observatory)

Abramenko, Astrophys. J. 629, 1141 (2005)

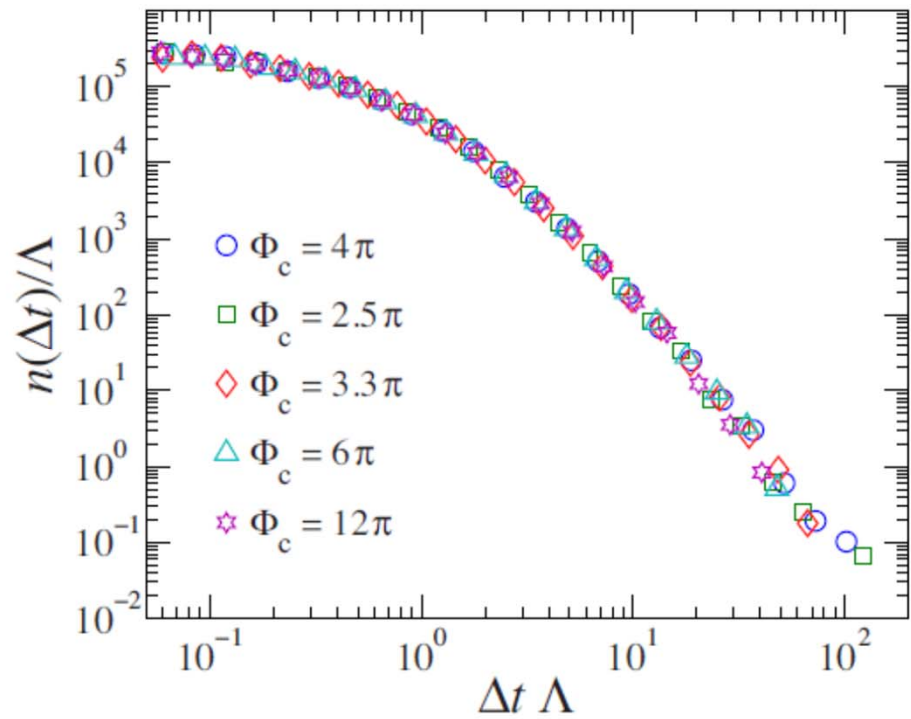
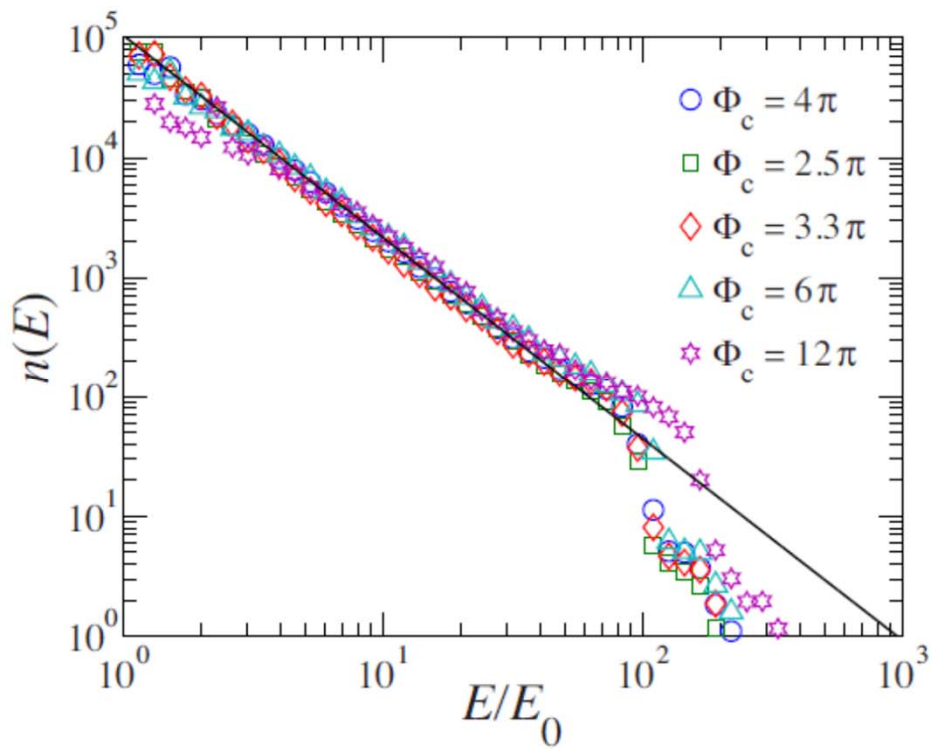
dependence on induced exponent γ

$$L = 512, N = 400, r_c/R = 0.1, \lambda < 1$$





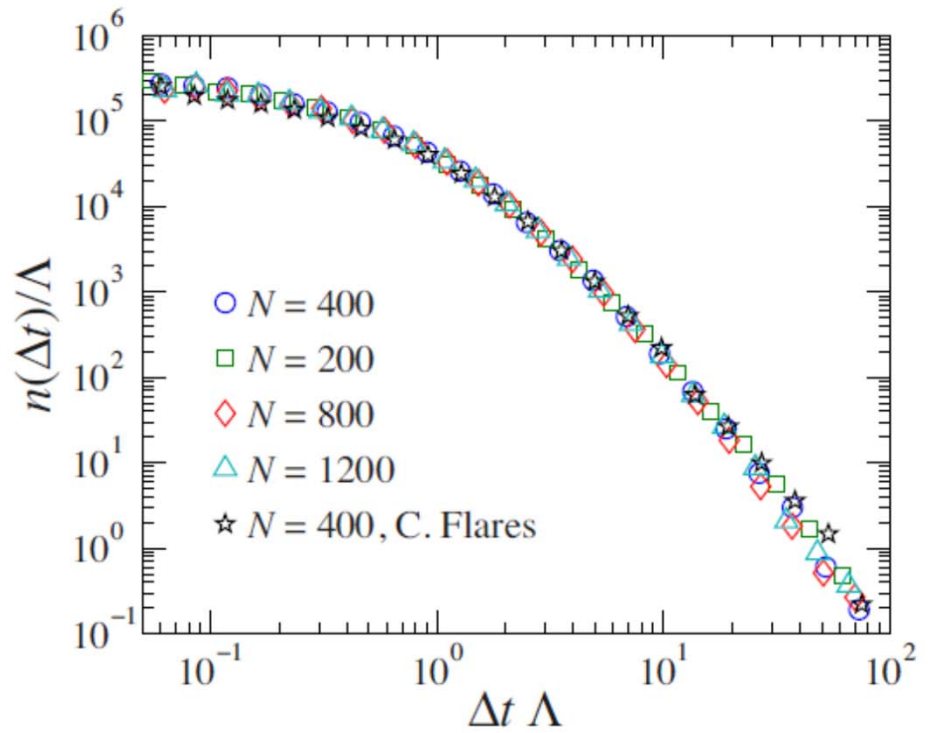
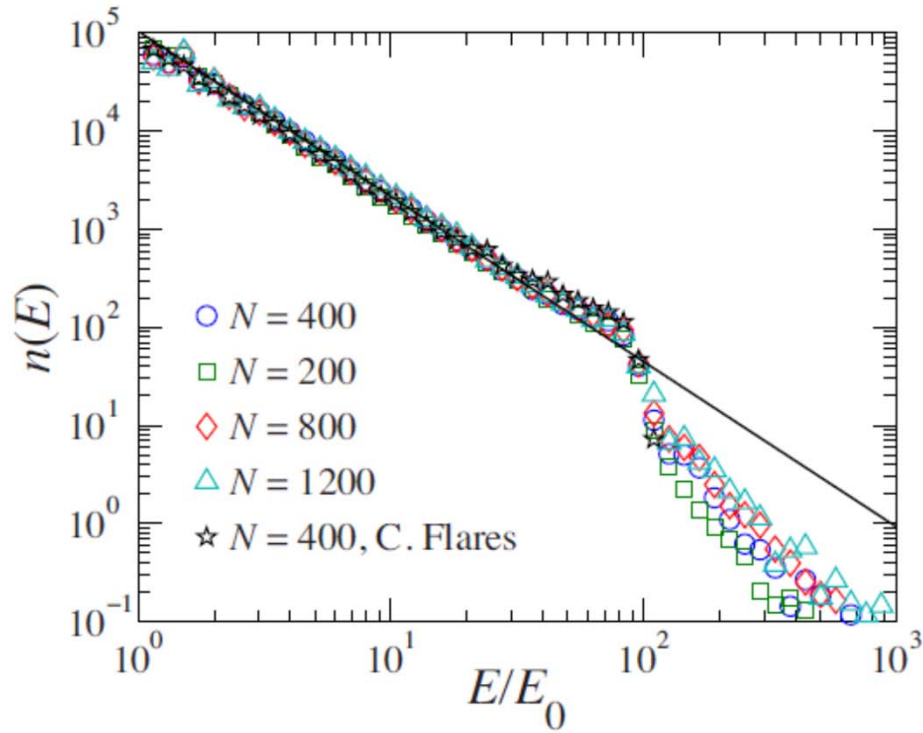
dependence on critical twist Φ_c



$L = 512, N = 400, r_c/R = 0.1, \lambda < 1$



dependence on density

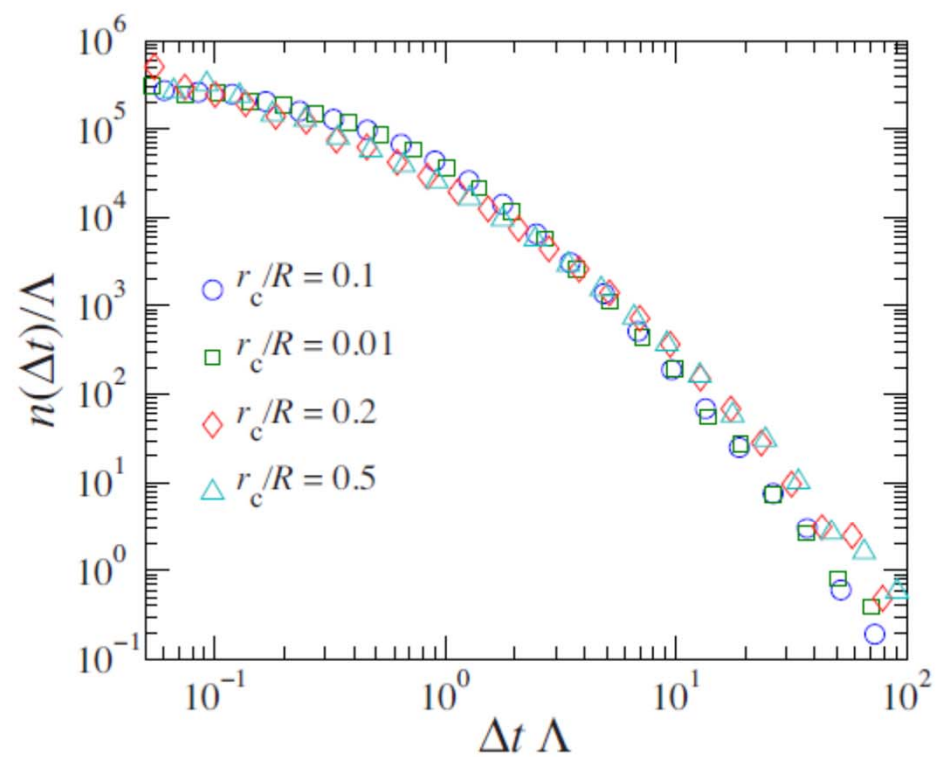
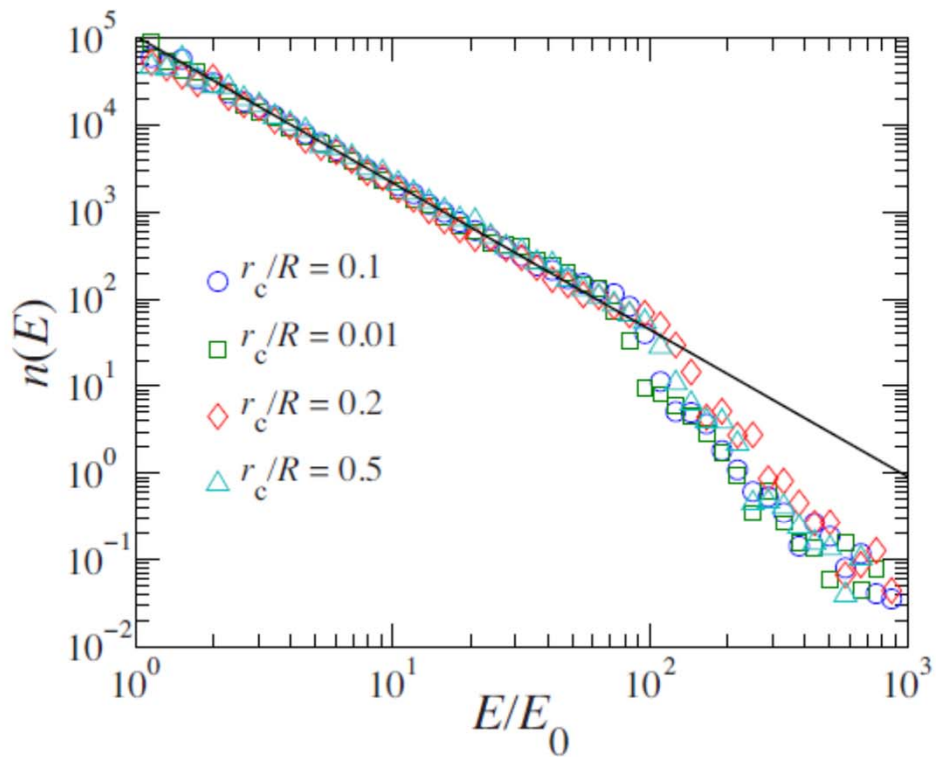


N = number of loops

$L = 512, r_c/R = 0.1, \lambda < 1, \Phi_c = 4\pi$



dependence on aspect ratio of flux tube



$L = 512, N = 400, \lambda < 1, \Phi_c = 4\pi$



Conclusion

- Energy distribution is ruled by the turbulent features of the flow in the photospheric plasma and not through a SOC-like mechanism.
- Interaction between flux tubes is necessary to obtain the observed waiting time distribution.
- Interactions that do not generate avalanches reproduce better the observed correlations between time and energy.
- SOC models fail to reproduce the power-law of the waiting time distribution.
- Solar flare statistics can not be described by SOC.